Effects of fly ash on the oxidation of mercury during post-combustion conditions

by

Hongqun Yang

A dissertation submitted to the graduate faculty

in partial fulfillment of the requirements for the degree of

DOCTOR OF PHILOSOPHY

Major: Chemical Engineering

Program of Study Committee:
Robert C. Brown, Major Professor
Kenneth M. Bryden
Gerald M. Colver
Douglas W. Jacobson
Dean L. Ulrichson
Thomas D. Wheelock

Iowa State University

Ames, Iowa

2002

Graduate College

Iowa State University

This is to certify that the doctoral dissertation of

Hongqun Yang

has met the dissertation requirements of Iowa State University

Signature was redacted for privacy.

Committee Member

Signature was redacted for privacy.

Committee Member

Signature was redacted for privacy.

Committee Member

Signature was redacted for privacy.

Committee Member

Signature was redacted for privacy.

Committee Member

Signature was redacted for privacy.

Major Professor

Signature was redacted for privacy.

For the Major Program

TABLE OF CONTENTS

LIST OF FIGURES

LIST OF TABLES

ACKNOWLEDGEMENTS

I would like to thank Dr. Robert C. Brown for this research opportunity to practice and enhance my knowledge. Thanks for his guidance through my research and dissertation writing. I also want to thank Glenn A. Norton for sharing his expertise of mercury chemistry and his assistance with experiments. Special thanks go to my committee members Dr. Kenneth M. Bryden, Dr. Gerald M. Colver, Dr. Douglas W. Jacobson, Dr. Dean L. Ulrichson and Dr. Thomas D. Wheelock for serving on my committee.

Thanks Dr. John Erjavec for performing the statistical analyses. Thanks Dr. Maohong Fan for performing the total organic carbon analyses on the fly ash samples. Thanks Dr. Joseph M. Okoh for performing the BET analyses. Thanks Grant E. Dunham, Dennis L. Laudal and Jerod L. Smeenk for their technical assistance. Thanks Diane M. Love and Tonia M. McCarley for their administrative assistance on this research project.

Finally, I want to thank my family for their invaluable support.

ABSTRACT

Mercury emissions from coal-fired power plants pose impact on human health. The emissions will be regulated in the near future. Mercury speciation in flue gas has an important effect on the efficiency of mercury emission control devices. This study focuses on the role of fly ash on the oxidation of Hg^0 in bench-scale simulated flue gas environment and in laboratory-scale coal combustion flue gas environment. The effects of flue gas matrices, temperature, fly ash mineralogy and morphology on the oxidation of Hg^0 are studied. Conclusions are drawn based on the testing results:

- Mercury chemistry is very complex in flue gas.
- The presence of fly ash is critical for heterogeneous Hg^0 oxidation.
- The flue gas components, including NO_2, HCl, NO and SO_2, have strong effects on the potential of whole fly ashes to oxidize Hg^0.
- Fly ash specific surface area appears to have a determining effect on Hg^0 heterogeneous oxidation.

CHAPTER 1. INTRODUCTION

This study focuses on the oxidation of Hg^0 by fly ash in the post-combustion environment. The effects of varying concentrations of HCl, NO_x, SO_x and moisture on the oxidation of Hg^0 are studied.

The 1990 Clean Air Act Amendments (CAAA) listed 189 pollutants as hazardous or toxic, collectively known as "air toxics". Title III of the 11 titles contained in CAAA motivated research initiated by Electric Power Research Institute (EPRI) and the U.S. Department of Energy through the Federal Energy Technology Center (DOE/FETC) to sample and analyze the listed 189 Hazardous Air Pollutants (HAP) from various sources in 1990 through 1997. As a result, many databases were developed on air toxic emissions from all industry stationary sources in the United States. Analyzing these data revealed that elements not collected at high efficiency were Hg, Se and As [1]. Among these "toxics", mercury is believed to pose the most significant impact on human health. On December 14, 2000, EPA decided mercury emissions from power plants must be reduced. It will propose regulations by December 2003, and issue final rules by December 2004. When fully implemented in 2005, the rules will reduce the human activity caused mercury emission by nearly 50% from 1990 levels nationwide [2].

Mercury emissions vary from site to site, mainly due to different boiler configurations, air pollution control devices (APCD), coal types and operating conditions. Some mercury can be removed by existing APCDs. In order to control mercury emission effectively under a wide range of conditions, predictive models need to be built and supplied to process engineers to retrofit conventional APCD or design new processes.

Studies show mercury speciation is an important parameter affecting the mercury removal efficiency. A positive correlation has been established between the fraction of oxidized mercury and the mercury removal efficiency [1,13]. Oxidized mercury (Hg^{2+}, Hg^{+}) tends to be removed by wet or dry flue gas desulfurization device (WFGD/FGD). Data collected by DOE/FETC and EPRI indicate that the flue gas from a power plant utilizing WFGD contained 80-95% oxidized mercury before entering the scrubbing device. After passing through the WFGD, 50-65% of the total mercury was removed. The data also show that plants utilizing WFGD burn bituminous coals that contain medium to high-sulfur contents [1]. The flue gas from these facilities has the highest concentrations of oxidized mercury upstream of WFGDs. For boilers firing subbituminous coals, collected data show 20-30% mercury capture with electrostatic precipitators (ESP), and 50-60% mercury capture with baghouse collection. High concentrations of elemental mercury present in flue gas are common in plants firing Powder River Basin (PRB) coal and other subbituminous coals [1].

The mercury concentration in coal varies. Literature data show a wide range of concentrations from undetectable levels to 0.206 ppmw for some commonly used coal in the U.S.. The average mercury reduction from coal cleaning is 30% on a mass basis [1]. Mercury in coal is released during combustion high temperature furnace section as elemental mercury. Hg^0 is then oxidized in an environment containing CO, CO_2, NO_x, SO_x, HCl, H_2O and fly ash as temperature cools down.

Some research clearly shows that homogeneous oxidation pathways exist [3,4,5]. Heterogeneous oxidation is also believed to be important in some conditions, either promoting direct oxidation or catalytically converting Hg^0 to Hg^{2+} [6]. Without incorporating

flue gas–Hg–fly ash heterogeneous interactions, mercury oxidation predicted by some thermodynamics models is much lower than the data from experiments [7,8].

A manual wet-chemical sampling train (Ontario–Hydro method) is utilized to sample flue gas for measuring mercury speciation in our research [1]. This method is commonly agreed to have a promise for Hg speciation. The mercury species captured in the chemicals are then analyzed by conventional cold vapor atomic absorption spectroscopy (CVAAS).

Both bench-scale testing and laboratory-scale testing are performed. Particular attention is paid to the role of fly ash on the oxidation of Hg^0 in both simulated and coal combustion flue gas environments.

In the bench-scale testing, fly ashes from different types of coal are studied. Sized fly ash and magnetically partitioned fly ash are studied too. Fly ash chemical composition, morphology, mineralogy are studied using appropriate methods.

In the laboratory-scale testing, a 35-kW down-flow combustion reactor is used and it is equipped with two high efficiency baghouses for ash collection. This reactor is operated in such a manner that it provides a residence time comparable to that of a full-scale unit. HCl, NO_x, SO_x, CO_x are monitored using appropriate analyzers.

The resulting mercury speciation data are analyzed and presented. Fly ash characteristics, important flue gas components and operating conditions are identified. All these will help advance the understanding of the mechanisms of flue gas–Hg–fly ash interactions during the post-combustion conditions.

CHAPTER 2. BACKGROUND

Human exposure to mercury is mainly in two forms: the vapor of metallic mercury Hg^0 and methyl mercury compounds. Metallic mercury vapor can exist in the ambient atmosphere and some working environments. Methyl mercury is a neurotoxin and is the most toxic chemical form of mercury. Methyl mercury compounds exist in natural water bodies and consequently accumulate in tissues of fish and marine mammals. Fish consumption and breathing the polluted air cause mercury bioaccumulation in human body and raise health concerns [20].

Anthropogenic mercury emissions account for ~10-30% of the total mercury emissions. EPA estimated that annual emissions of mercury from human activities in the U.S. were 159 tons during the period of 1994-1995. Approximately 87% of these emissions were from combustion sources. Coal-fired utilities in the U.S. were estimated to emit 51 tons of mercury into the air during this period. Both elemental and oxidized mercury are emitted to the air from combustion facilities. Elemental mercury in the atmosphere has a lifetime of up to a year, while oxidized forms of mercury have a lifetime of a few days or less as a result of the high solubility of Hg^{+2} in atmospheric moisture. Elemental mercury can thus be transported over long distances, whereas oxidized and particulate mercury deposits near the point of emission. Once mercury has deposited on land or water, it can be transformed into methyl mercury, and enter the food chain [7].

Hg speciation in flue gas has a significant impact on the design strategies for capturing Hg emissions. Oxidized mercury is water-soluble and may be removed in conventional acid gas scrubbers used for SO_2 control. However, Hg^0 is insoluble in water and

must be adsorbed onto a sorbent or converted to a water-soluble form that can be collected by wet scrubbing devices. Thus oxidized forms of mercury are preferred from the point of view of mercury control.

Mercury is present in coal at low concentrations on the order of 0.1 ppmw. In the combustion zone of a coal-fired boiler, all the mercury in the coal is vaporized as elemental mercury, yielding vapor mercury concentration in the range of 1 to 20 $\mu g/m^3$ (1 to 20 ppbw). At furnace exit temperature (1700 K), all the mercury is expected to remain as the thermodynamically favored elemental form in the flue gas. As the gas cools after combustion, oxidation reactions can occur, significantly reducing the concentration of elemental mercury by the time the post-combustion gases approach the stack [7].

Current measurement methods cannot identify specific oxidized species of mercury. The observed range of mercury concentration in flue gas is broad. Mercury oxidation mechanisms during the post-combustion conditions are complex and currently cannot be quantitatively described. Some thermodynamics models have been developed with limited application.

Several research efforts have investigated mercury speciation due to gas-phase reactions. Earlier investigation undertaken by Hall et al. studied the effects of HCl, Cl_2, NO_x, and O_2 on Hg speciation. The results indicate that the concentration of HCl in the flue gas significantly affects the oxidation of Hg^0. Temperature has some effect too [8].

Research performed by Sliger et al. indicates that the dominant oxidizing species in flue gas is Cl-atom, which reacts with Hg^0 during quenching of flue gas. Key parameters proposed to affect Hg conversion are Cl-atom and Cl_2 concentrations in the flue gas, the flue gas quenching rate, and the rate at which Cl-atoms recombine into Cl_2.

Some previous research has been done to investigate the effects of fly ash on the mercury speciation during the post-combustion conditions. Key parameters of fly ash include mineralogical composition, morphology, specific surface area, total organic carbon (TOC) and loss-on-ignition (LOI).

Fly ash from certain types of coal appears to have the ability to catalyze the oxidation of Hg^0. The reasons have not been identified. The TOC in fly ash is an important factor that has not been thoroughly investigated. The TOC could possibly be involved in the oxidation of Hg^0 and could collect some of the Hg in flue gas.

Oxidized Hg is more easily captured by carbon than Hg^0 (g). A positive correlation has been observed between the Hg capturing efficiency by fly ash control device and the measured TOC in the fly ash. In one study [20], the retention of mercury by fly ash is studied by exposing a fabric filter (FF) loaded with fly ash to simulated flue gas containing Hg^0 at elevated temperature. The fly ash retains significant amount of mercury. The carbon content of the fly ash is a crucial factor determining mercury retention by fly ash.

It is found that Hg adsorption on fly ash and activated carbon is enhanced with increased levels of HCl and decreased levels of SO_2. The effect of fly ash surface is not sufficient to explain the adsorption of Hg onto fly ash and the oxidation of Hg^0. Flue gas chemistry needs to be considered. Some researchers proposed that active sites on the fly ash surface contribute to the oxidation and capturing of Hg. Other researchers studied the effects of pore size distribution and sulfur content of the fly ash.

Currently there is a need to develop economically viable technologies for controlling mercury emissions. Processes being developed commercially for capturing and removing mercury from coal-fired flue gas generally rely on one of the two approaches [27]:

- Adsorption on a solid sorbent; or
- Chemical conversion to a nonvolatile or water-soluble form.

Adsorption by activated carbon is primarily achieved by one of the two methods: flue gas injection of powdered activated carbon (PAC) up stream of a particulate control device (PCD), or installation of a fixed or fluidized bed carbon adsorption system downstream of a PCD. These sorbents adsorb vapor-phase mercury compounds and are collected in the PCD such as a fabric filter or an ESP. In order to optimize the operation of these devices on a large scale, understanding mercury speciation and flue gas–Hg–fly ash interactions is important.

2.1 Mercury and Coal

Mercury is associated primarily with the inorganic mineral components of coal, although an association with the organic maceral components of coal as organomercuric compounds also has been suggested. Mercury is classified geochemically as a chalcophile element [24].

Pyrite (FeS_2) and cinnabar (HgS) are the dominant mineral hosts for mercury in coal. As the mineral and possibly organomercuric hosts of mercury decompose during combustion (>1400 ^{0}C), mercury is liberated as Hg^0 (g) (boiling point of 357 ^{0}C at 1 atm, vapor pressure of 0.180 Pa at 20 ^{0}C). In contrast to the nonvolatile and semivolatile trace elements in coal, the mode of occurrence of mercury (i.e. mineral or maceral association) does not affect this initial combustion transformation mechanism.

Knowledge of the physical and chemical transformations of mercury in coal combustion flue gas is imperative for understanding the transport and fate of mercury

released into APCD and the atmosphere. Figure 1 presents the mercury transformations during the coal combustion process [24].

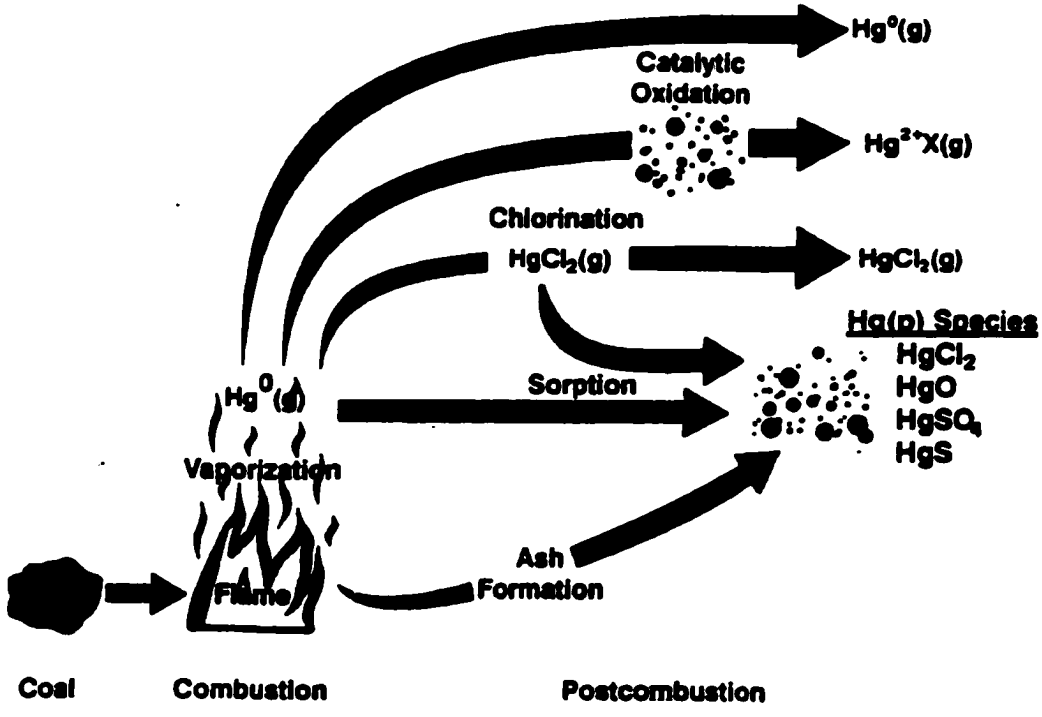

Figure 1. Mercury transformations during coal combustion process

The potential of mercury emissions from coal combustion varies considerably from site to site due to differences in coal compositions and combustion devices. It is well known that the chemical composition of coal is highly variable, even within a given seam. The measured concentrations of mercury are no exception, displaying variations that span several orders of magnitude. Bituminous and anthracite coals have the highest mean mercury concentrations of 0.21 ppmw and 0.23 ppmw, respectively [27]. However, a range of concentrations have been reported for bituminous coal from less than 0.01 ppmw up to 3.3

ppmw, and values as high as 8.0 ppmw have been reported for subbituminous coal. The fate of trace elements in the combustion process is influenced by the type of boilers, the operating conditions, and the APCD, as well as by the concentrations of other elements in the coal, such as Cl and N. Mercury belongs to a group of elements/compounds denoted as Class III, which remains primarily in the vapor phase throughout the boiler and subsequent APCD. However, mercury speciation can be influenced by reactions with other species. Only trace amounts of mercury present in coal-combustion flue gas. The concentration of mercury in the flue gas from the combustion of typical coals falls within a range of 5 to 70 $\mu g/m^3$.

Current knowledge of mercury transformations in coal combustion flue gas is based largely on thermodynamics modeling and experimental investigations of mercury reactions in simulated flue gases and, to a limited extent, on the interpretation of field test data. Mercury exists primarily as gaseous elemental mercury in the furnace, and as gaseous or solid inorganic mercuric compounds in combustion flue gas. Mercury emissions from coal-fired electric utility boilers can be empirically classified, based primarily on the capabilities of currently available analytical methods for determining mercury speciation, into 3 main forms: Hg (g), Hg^{2+} (g), and particulate mercury Hg (p), with a large range in the relative concentrations of Hg^0 (g), Hg^{2+} (g) and Hg (p) [24].

2.2 Fly Ash

Fly ash is a by-product of coal combustion. Differences in fuel composition and in boiler operating conditions lead to the complicated fly ash composition. Most fly ash consists of inorganic minerals and elemental carbon. Occasionally, fly ash contains small quantities of raw coal or volatile organic compounds [25].

During the coal combustion process, three parts of products are formed: flue gas, bottom ash and fly ash. Fly ash is the product that is entrained into combustion exhaust leaving the furnace and is collected in either mechanical collectors or ESPs. The flue gas is the product of the coal material that is oxidized or volatized during combustion process. The complex coal composition results in the diversity of fly ash characteristics. However, fly ashes can be categorized by their origin, chemical composition, physical composition and morphology.

Fly ash generally consists of inhomogeneous fine spherical particulates usually ranging in diameter from 0.5 μm to 100 μm with a color span from light tan to gray to black. Increased carbon content causes a darker gray-black appearance of fly ash, while increased iron content tends to produce a tan-colored or reddish fly ash. Particle size distribution and total surface area of fly ash vary depending on the types of fly ash collector equipment. The ash collected by ESPs contains a much greater percentage of the very small particles (<1.5 μm). The lithophite materials (aluminosilicates) are more concentrated in fine particles. The magnetite-hematite materials (iron-bearing) are more concentrated in the coarser particles. The alkalis (Na & K) are generally more concentrated in finer particles, probably because of their association with lithophites.

The highest LOI occurs in the finer particles. The most abundant component in fly ash, glassy compounds, is concentrated in the fly ash collected from ESP. Magnetite-hematite, the second most abundant constituent in fly ash, is also concentrated in the fly ash collected from ESP. Magnetite-hematite particles may also be found as small opaque inclusions in the glass particles.

Carbon in fly ash has various shapes with the predominant shape being highly irregular cellular particles. Carbon particles in the coarser fly ash have a cinder-like appearance and are magnetic because of the presence of particles of magnetite and hematite lodged in the cellular structure of carbon particle walls. The aggregates of glass, magnetite, hematite and carbon particles are present in all sizes of fly ash. X-ray diffraction studies show that crystalline constituents are hematite, quartz mullite and anhydrite.

Fly ash is rich in the following elements: Si, Hg, Cl, Sb, F, Se, V, Pb, Mo, Ni, B, Zn, Cd, Cr, Cu, Co, U, As and Ag. Elements that are approximately equally distributed in the bottom ash and fly ash include Ba, Be, Fe, Al, Ca, T, Mn and Mg.

The specific surface area of fly ash particles is an important parameter in determining a number of the behavioral characteristics of coal fly ash. It is the surface area of a particle that determines the number of electrostatic charges that can be placed on that particle in an electrostatic precipitator, the extent of condensation or adsorption of species from the gas phase, and the rate and extent of its aqueous leaching [21].

To a reasonable approximation, one would expect the specific surface area of fly ash to increase linearly with decreasing particle size since the particles are predominantly spherical. Similar trends would also be expected for nonspherical particles having similar shape factors. Sometimes, fly ash shows no significant dependence of surface area on particle

size, especially for small particles. This indicates the existence of substantial internal surface area that is effectively proportional to particle volume rather than the external surface area [21].

Morphology studies by light and electron microscopy have described the heterogeneity and structural complexity of fly ash. Based on morphological appearance, much can be inferred concerning origin, formation, and chemical composition. Light microscopy has been used to define major morphological classes of coal fly ash particles based on particle shape and degree of opacity. SEM-X-ray analysis is used to define the crystal structure in the fly ash. Transmission Electron Microscopy (TEM) and Electron-Diffraction Analysis are used to study mineral composition and structure [21].

2.3 Flue Gas–Mercury Interactions

In a kinetic modeling study, Senior et al. utilize SOLGASMIX to conduct equilibrium calculation for a combustion process [7]. Chlorine-containing species have been shown to be the most important for oxidation of elemental mercury in flue gas. Other flue gas components (H_2O, SO_2, NO_2, etc.) may have secondary effects on the rate of homogeneous oxidation of mercury. The conversion of HCl to Cl_2 in the flue gas of a coal-fired power plant is kinetically limited. Both homogeneous and heterogeneous reactions may contribute to mercury oxidation in coal combustion systems.

In another study of a chemical kinetic modeling [13], Sliger et al. suggests the important mercury oxidation paths are:

$$Hg + Cl \leftrightarrow HgCl \qquad (2\text{-}1)$$

$$HgCl + Cl \leftrightarrow HgCl_2 \qquad (2\text{-}2)$$

The Cl-atom is derived from high-temperature (1085~922 ^{0}C) dissociation of HCl:

$$OH + HCl \leftrightarrow Cl + H_2O \qquad (2\text{-}3)$$

During thermal quenching of the gases, recombination of Cl-atoms to Cl_2 is kinetically limited, the resulting super-equilibrium of Cl-atoms leads to the oxidation of mercury as the quench proceeds to the lower temperatures where the decomposition of $HgCl_2$ is suppressed. The homogeneous oxidation is governed by:

- HCl concentration as a source of Cl-atom;
- Quenching rate;
- Background gas composition.

Based on the work of Sliger et al., another group of researchers proposed a more complex Hg oxidation model consisting of 18 steps of reactions [8]. This model predicts that substantial Hg conversion only happens during quenching of the flue gas. At lower temperature (less than ~630 ^{0}C), the model predicts insufficient amount of Cl-atom and Cl_2. This model drastically under-predicts the mercury conversion trends. The performance of this model improves at higher temperature, and it correctly predicts the effects of increased HCl concentration on increased mercury conversion. The model predicts increased mercury conversion with increasing gas moisture content. Three of the important reactions are listed here:

$$Hg + Cl \leftrightarrow HgCl \qquad (2\text{-}4)$$

$$HgCl + Cl \leftrightarrow HgCl_2 \qquad (2\text{-}5)$$

$$Hg + Cl_2 \leftrightarrow HgCl_2 \qquad (2\text{-}6)$$

They propose that Hg conversion is dictated by the interplay between the initiation step (reaction 2-4) and the Cl-atom recombination reaction (reaction 2-7). Cl-atom concentration is the rate-determining factor.

$$2Cl \leftrightarrow Cl_2 \qquad (2\text{-}7)$$

High HCl concentrations are required at temperatures above 973 K to obtain measurable mercury oxidation from homogeneous gas phase reaction chemistry. Chlorine species are the primary oxidants in coal combustion, with molecular chlorine being more effective than HCl [32].

Molecular chlorine has been studied as an important gas phase oxidative reactant for elemental mercury in post-combustion gases [32]. Also reported is the fast and complete reaction of mercury and molecular chlorine to produce $HgCl_2$ in a constant temperature flow reactor, and in a variable temperature flue gas reactor at temperatures ranging from ambient to above 973 K. Hall et al. studied reactions under conditions of decreasing temperature as well as under isothermal conditions, observing a dependence on chlorine concentration, with 25% conversion observed at 10 ppm Cl_2 and 70% conversion at 150 ppm Cl_2 at 773 K.

Experiments with Cl_2 demonstrate that nearly complete conversion could be obtained at sampling temperatures of 773 K and post-flame cooling rates of 400 K/s in the presence of high chlorine concentrations (500 ppm). Decreasing chlorine concentrations lead to decreasing mercury conversion [32].

2.4 Flue Gas–Hg–Fly Ash Interactions

A review of mercury transformations in coal combustion flue gas highlights the importance of heterogeneous interactions in controlling Hg^0 (g) to $Hg^{2+}X$ (s, g) conversions at high temperature [24]. Mercury chlorination is assumed to be the dominant transformation mechanism. Other potential mechanisms involve mercury interactions with fly ash surfaces where reactive chemical species, oxidation catalysts, and active sorption sites are available to transform Hg^0 (g) to HgX (g) as well as transform Hg^0 (g) and $HgCl_2$ (g) to Hg (p). From the investigation of Hg^0(g)-O_2(g)-HCl(g) interactions and Hg-HCl(g)-fly ash interactions in a 42-MJ/hr combustion reactor, the following observations and conclusions are made:

- A Hg^0(g)-O_2(g) reaction catalyzed by Al_2O_3 (s) and TiO_2 (s) components in the refractory is postulated. HgO (g) is the suspected reaction product, although mercury nitrite or nitrate species could be an intermediate.
- The effects of HCl (g), CaO (s), fly ash mineralogy as well as crystal chemical considerations suggest that ferrite spinel is the dominant mercury host in the Hg(p)-enriched fly ash.
- Low recoveries of mercury during 100-ppmv HCl injections into the simulated flue gas (consists of 8.5 mol% O_2, 91.5 mol% N_2) and the PRB coal combustion flue gas suggest that $HgCl_2$ is formed and adsorbed onto insulating components of the combustion reactor.

A fixed-bed study of the interactions between mercury and sixteen different fly ash samples performed by Dunham [28] et al. reports that only a general trend of increased oxidation and capturing of the oxidized mercury with increasing LOI and surface area but no

strong correlation. The capturing increases with decreasing temperature, this indicates physi-sorption occurs. Similar results are generated from testing with $HgCl_2$ injection. There is no correlation of elemental mercury capturing with LOI, surface area or ash type.

Galbreath et al. reports that CaO (s) is an important Hg-sorption component of a subbituminous fly ash [22]. HCl (g) is scavenged by ash particles and the formation of particle-associated Cl-atom inhibits Hg-fly ash sorption. 50% of the spiked Hg^0 is oxidized through a possible catalyzed $Hg^0(g)$–$O_2(g)$ reaction involving a refractory metal oxide compound. It is suggested that $HgCl_2$ (s, l) is formed in their combustion system [22].

Lee et al. [23] perform a study of four-component and three-component simulated fly ashes under simulated flue gas conditions:

- The three-component fly ash consists of: 62 wt.% Al_2O_3, 24 wt.% SiO_2 and 14 wt.% Fe_2O_3.
- The four-component fly ash consists of: 18 wt.% Al_2O_3, 63 wt.%SiO_2, 13 wt.% Fe_2O_3 and 6 wt.% CaO.

Hg oxidation is studied by exposing the simulated fly ash to the simulated flue gas consisting of 2% O_2, 5% CO_2, 50-ppmv HCl, 40-ppbv elemental mercury and the balance N_2.

Both the three-component and four-component fly ashes exhibit identical final steady-state Hg^0 oxidation capabilities. However, the final steady-state oxidation over the four-component fly ash is achieved more slowly, with a longer induction period. The induction period may be due to the capture of HCl by CaO, where less HCl is available for the production of chlorinating agent(s) to oxidize Hg^0, thus causing an induction period of Hg^0 oxidation over the four-component fly ash. Also found are the combined inhibition effects of SO_2 and H_2O on Hg^0 oxidation. Lee et al. reported that NO_x are the active

components in the flue gas for the oxidation of Hg^0. NO_x are more active than HCl. In the presence of NO_x, components such as alumina (Al_2O_3) and silica (SiO_2) are active for the oxidation of Hg^0. The catalytic activity of Blackville fly ash may be related to the Fe_2O_3 [23].

Examination of five different coal fly ash samples obtained from pilot combustion facilities reveals a positive correlation between iron content of coal fly ash and oxidized mercury concentration. In the presence of HCl, the most likely product is $HgCl_2$. In the presence of NO_x, the most likely product is $Hg(NO_3)_2 \cdot H_2O$.

Bench-scale investigations by Galbreath et al. indicate that NO, NO_2 and hematite (α-Fe_2O_3) promote the conversion of gaseous elemental mercury (Hg^0) to gaseous oxidized mercury (Hg^{2+}) in simulated flue gas. In a study utilizing a coal combustion system, NO_x (80-190 ppmv) and (α-Fe_2O_3) are injected into the coal combustion flue gases derived from burning bituminous Blacksville, subbituminous Absaloka, and lignitic Falkirk coals in a 7-kW combustion system. Injections do not affect the Hg speciation in Absaloka and Falkirk coal combustion flue gases. An abundance of Hg^{2+} presents in Blacksville coal flue gas and magnetite (γ-Fe_2O_3) rather than hematite (α-Fe_2O_3) presents in the Blacksville coal fly ash. This indicates that (γ-Fe_2O_3) catalyzes mercury oxidation in the combustion testing [31].

Lee et al. [12] investigate the effects of iron content on the oxidation reactivity for a low-iron-content subbituminous coal fly ash and a lignite fly ash. After adding Fe_2O_3 to these two samples to reach the iron content similar to that of the Blacksville fly ash, significant Hg^0 reactivity is measured for these two iron-doped samples. However, the low-iron-content Valmont sample without iron doping is found to have high Hg^0 oxidation reactivity similar to that of the high-iron-content Blacksville sample. Effects of iron content are not clear.

2.5 Mercury Analyzer

Currently, there are several techniques to measure elemental mercury directly: Cold Vapor Atomic Absorption Spectroscopy (CVAAS), Cold Vapor Atomic Fluorescence Spectroscopy (CVAFS), as well as the emerging technology of chemical microsensors. CVAAS and CVAFS are the two commonly used techniques.

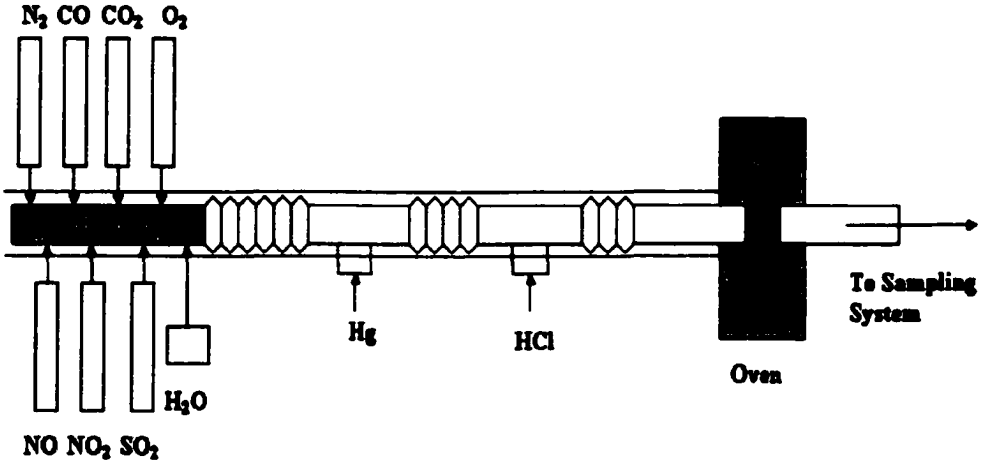

(a) Layout of the bench-scale system

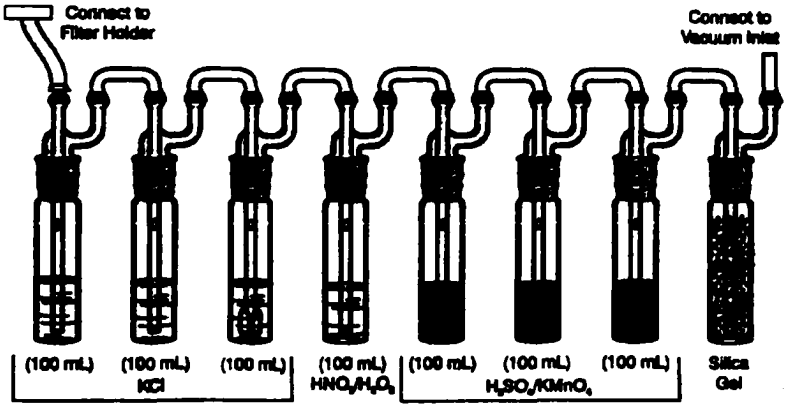

(b) Diagram of the Ontario-Hydro impinger train

(c) Photograph of the bench-scale system

Figure 2. Bench-scale system

CHAPTER 3. EXPERIMENTS

This research project consists of two parts: bench-scale testing and laboratory-scale testing: The bench-scale testing aims at studying the effects of fly ash on the oxidation of mercury using simulated flue gas. The laboratory-scale testing studies the speciation of mercury in the flue gas from a 35-kW down-flow combustion reactor burning PRB subbituminous coal or Blacksville bituminous coal.

3.1 Bench-Scale Testing

3.1.1 Bench-scale testing apparatus

A bench-scale testing apparatus was constructed to simulate coal-fired flue gas and to evaluate the effects of fly ash on the Hg speciation under the simulated flue gas conditions. This bench-scale system consists of a stainless steel mixing manifold, a gas humidification system, a convection oven for heating fly ash samples to the desired temperature, a series of impingers with absorbing solutions for collecting mercury species, and finally a dry gas meter. The bench-scale system components are shown in Figure 2.

The sample line carrying blended gases downstream from the manifold consists of corrugated TEFLON tubing wrapped with silicone heating tapes. All gases except for Hg^0 vapor and HCl are introduced into the mixing manifold to produce a gaseous mixture. The HCl and Hg are introduced downstream of the manifold via TEFLON tees connecting the sample transport line. The conduit from the mixing manifold up to the sampling impingers is constructed of TEFLON. The manifold and gas transport line are heated to desired

temperature. The gas stream is transported from the manifold to a convection oven containing a filter holder that exposes fly ash samples to the gas flow. Gas flow exiting the convection oven enters the mercury sampling impingers. The mercury is captured in the impinger solution. Speciation data are obtained by analyzing the solutions with a Leeman Labs PS200II mercury analyzer. The convection oven is a Linderberg/BlueM GOB10A/GO131OSA. This oven is designed to operate at temperature up to 260 ^{0}C.

Fly ash samples are loaded onto Whatman 9-cm diameter QMA quartz fiber filters using a Method 5 filter holder connected to a section of 1/8" stainless steel tubing. The downstream side of the filter holder is connected to a vacuum pump. For each testing, 0.6 g of ash is spread out into a thin layer on a clean, flat surface. The ash is suctioned up into the filter holder at a gas flow rate of 15 L/min. This gives an ash loading of 10 mg/cm^2. Different fly ash loadings and suction gas flow rates are tried, this loading gives the most even ash distribution.

The mercury generation system consists of Hg permeation cell, a housing U-tube, a water bath and transport line. A certified elemental Hg permeation tube from VICI Metronics is used to generate the elemental mercury vapor. The certified Hg^0 emission rate from the permeation tube is 175 ± 5 mg/min at 70.0 ^{0}C. The permeation tube is immersed in a VICI Metronics U-tube, which is heated in a covered water bath. The water bath is a Lindberg/BlueM constant temperature water bath. The model number is WB1110A. It's capable of automatically controlling temperature with an accuracy of ± 0.1 ^{0}C. It is run slightly hotter than the temperature set point, which results in slightly elevated Hg emission rates. Therefore, the actual mercury emission rate at the set point temperature is

experimentally determined by bubbling the gas into absorbing solutions over a period of time and then analyzing the absorbing solutions for mercury content. Actual mercury emission rate is determined to be 190 ng/min by this method. A stream of nitrogen flow of 200 ml/min continuously passes over the permeation tube and transports the Hg^0 vapor to the main gas line, where it is introduced into the simulated flue gas stream through a TEFLON mixing tee.

Table 1. Composition of the 15 L/min full blend and baseline simulated flue gas*

Gas Component	Concentration (mole) - Full Blend	Concentration (mole) - Baseline Blend
CO	100 ppm	100 ppm
CO_2	12 %	12 %
HCl	50 ppm	-
H_2O	10 %	10 %
NO	300 ppm	-
NO_2	20 ppm	-
O_2	6 %	6 %
SO_2	1600 ppm	-
N_2	Balance of 15 L/min	Balance of 15 L/min

* Always maintain dry gas flow rate of 15 L/min.

* Hg^0 vapor is introduced into the simulated flue gas at 190 ng/min.

The moisture generation system consists of de-ionized (DI) water supply, a dosing pump, and water vaporization coils immersed in heating oil. The oil is contained in a metal beaker heated by a Glas-Col-700 heating mantle. A stream of nitrogen flowing at 2 L/min carries the moisture through heated transport line into the primary gas stream. The desired moisture content is 10 % on a volumetric basis. The water pump is a MILTON ROY series 9A electronic metering pump with a stroke frequency from 0 to 100 SPM and the corresponding water flow rate is from 0~126 ml/min. Normal concentration of the gases used

in the simulated flue gas matrix is shown in Table 1. Compressed gas cylinders are used for the CO, CO_2, HCl, NO, NO_2, O_2, SO_2 and N_2. Certified HCl gas of a concentration accuracy of ±5% was purchased from Scott Special Gases. Certified NO, NO_2, SO_2, CO were purchased from Air Products and Chemicals, Inc.. The NO and NO_2 gases are metered by AALBORG mass flow controllers, model number AFC 2600D with an accuracy within ±1.0% full scale.

Concentrations of total, elemental, and oxidized Hg downstream of the ash samples are determined using Ontario-Hydro method. This method utilizes a condensing/absorbing system, including eight impingers immersed in an ice bath and connected in series with leak-free noncontaminating ground glass fittings. The first, second, forth, fifth, sixth, and eighth impingers are of Greenburg-Smith design modified by replacing the standard tip with a 1.3-cm-inner-diameter straight glass tube extending to about 1.3-cm above the bottom of the flask. The third and seventh impingers are also Greenburg-Smith design, but with a standard tip and a glass impinging plate. The first, second, and third impingers contain aqueous 1N potassium chloride (KCl) solution. The forth impinger contains aqueous solution of 5% v/v nitric acid and 10% v/v hydrogen peroxide (H_2O_2). The fifth to seventh contain aqueous solution of 4% w/v potassium permanganate ($KMnO_4$) and 10% v/v sulfuric acid. The last impinger contains silica gel or an equivalent desiccant. The Ontario-Hydro apparatus is shown in Figure 2.

The mercury collected in the first, the second and the third impingers represents Hg^{2+} while the mercury collected in the forth to seventh represents Hg^0. The purpose of the HNO_3/H_2O_2 is to absorb SO_2, thus protecting the acidified permanganate solutions. The sum gives total mercury. After passing the gas mixture through the Ontario-Hydro apparatus for

75 minutes unless otherwise specified, the solutions from these impingers are then treated following a series of steps and finally analyzed by a Leeman Labs PS200II mercury analyzer using CVAAS principal. Each test is repeated once. As a step for quality control, a blank test of 15 L/min N_2 mixed with Hg^0 vapor passing through the Ontario-Hydro apparatus with all other conditions identical is run to see that everything is working properly.

3.1.2 Bench-scale testing approaches

After fly ash is loaded onto the quartz filter, a filter housing is installed to hold the loaded filter. The housing is placed in the convection oven, which is then heated to the desired temperature. A continuous stream of blended gas containing elemental Hg is passed through the fly ash at a total dry gas flow rate of 15 L/min for a period of 75 minutes. In addition to using the full gas blend, some tests are performed using only a baseline blend consisting of CO, CO_2, Hg, N_2, O_2 and H_2O. The baseline blend is assumed to be nonreactive. Other tests involve adding specific reactive gases or combinations of reactive gases to the baseline blend. The reactive gases are HCl, NO, NO_2 and SO_2. When some of the gases in the simulated flue gas are eliminated to provide the desired matrix for specific tests, the flow of the N_2 balance gas is increased accordingly to maintain the 15 L/min nominal flow rate. All tests are performed at least in duplicate, and fresh fly ash samples are used for each test. Prior to each test, the gases are allowed to equilibrate the bench-scale system. With the exception of Hg and HCl, the gases are allowed to equilibrate for a period of at least 1 hour. The HCl stream is allowed to equilibrate for two hours, while the Hg stream is allowed to equilibrate over night prior to testing.

The full factorial design testing is performed to determine the effects of gas matrices on mercury oxidation. Tests are initially performed with the whole PRB and whole Blacksville fly ash samples using both the baseline blend and the full blend gas. These tests are performed at 120 ^{0}C and 180 ^{0}C. As a reference point and a quality control measure, tests are also performed using the full gas blend with blank filters. In addition, a limited number of tests with magnetic and nonmagnetic concentrates from the unsized Blacksville fly ash are performed using the full blend gas at 180 ^{0}C.

Other tests are performed at 180 ^{0}C using sized PRB fly ash (first and second cyclone catches only) and whole Blacksville fly ash, as well as magnetic and nonmagnetic concentrates from the sized Blacksville fly ash. PRB fly ash does not contain any highly magnetic material. Similarly, magnetic concentrates are not available for the Blacksville fly ash from the second cyclone catch. For the Blacksville fly ash, the sized ash fractions are also exposed to various combinations of gases at 180 ^{0}C. In particular, tests are performed using the baseline blend with various gases added:

- NO_2,
- NO_2 + HCl,
- NO_2 + SO_2,
- NO_2 + SO_2 + HCl.

3.2 Fly Ash Sample Characterization

A particle sizing system consisting of 3 cyclones is used to separate the fly ash into different sizes. Fly ash caught in cyclone 1 has a nominal size greater than 10 μm, fly ash

caught in cyclone 2 has a nominal size from 3 μm to 10 μm; cyclone 3 catches particles with a nominal size less than 3 μm.

In our study, magnetic force is used to separate Blacksville fly ash into magnetic/medium-magnetic/nonmagnetic fractions. Blacksville fly ash consists of 19 wt.% magnetic fraction, 41 wt.% medium-magnetic fraction and 40 wt.% nonmagnetic fraction. PRB fly ash consists of only nonmagnetic material.

Scanning electron microscopy with energy dispersive X-ray analysis (SEM-EXD) is used to examine the morphology and chemical composition of the fly ash samples. A HITACHI S-2460N SEM is used with an Oxford Instrument Isis Model 200 X-ray analyzer. This analysis gives fly ash composition at the spot targeted by an electron beam with an effective scanning depth on the order of 1 to 2 μm. The resulted qualitative chemical composition of a fly ash sample has an accuracy of about 20%.

Coal combustion fly ash typically contains a considerable amount of crystalline material. X-ray diffraction (XRD) is used to examine the mineralogical composition of the whole and fractionated fly ash samples. The scans are performed using a SIEMENS D500 X-ray diffractometer with Cu K-α radiation.

BET N_2 adsorption isotherms are obtained on whole fly ash, mechanically sized fly ash and magnetically fractionated fly ash samples with a Miromeritics Instrument Corporation Accelerated Surface Area Porosimeter 2010.

TOC in fly ash samples is determined using a Perkin Elmer TGA7 Thermogravimetric Analyzer with a TAC 7/DX controller. About 25 mg of ash is heated to 750 ^{0}C at a rate of 20 ^{0}C/min in N_2. The sample is held at that temperature until a constant weight is obtained, which takes about 30 minutes. The gas stream is then switched to air

while maintaining a temperature of 750 ^{0}C. The weight loss observed in the presence of air is measured, which constitutes the TOC of the sample.

3.3 Laboratory-Scale Testing

The laboratory-scale system consists of a 35-kW down-flow combustion reactor, two pulse baghouses equipped with TEFLON fabric filter, pneumatic coal conveying system, gas sampling system and data acquisition system. Refer to Figure 3, Figure 4 for diagrams of the laboratory-scale system.

3.3.1 Design of the down-flow combustion reactor

This 35-kW down-flow combustion reactor was designed to handle a variety of fuels. Natural gas and pulverized coal are used in this study. Natural gas is used to heat the combustion reactor to combustion temperatures after which the combustion of coal is self-sustaining. Two sections of the combustion chamber are optional and can be added or removed to control the residence time.

The laboratory-scale combustion reactor consists of a natural gas burner, a modular combustion chamber, a pneumatic injection system to transport the pulverized coal powder into the combustion feeding zone, a gas sampling system to sample flue gas and filter the moisture and particulates of the sampled gas stream, and gas analyzers to determine CO, CO_2, NO_x and SO_2 concentrations.

3.3.2 Natural gas burner and controller

The natural gas burner is a Kromschroder BIC-50. The nozzle-mixed burner is nominally rated at 35 kW. The gas mixture is ignited through direct spark ignition by a Kromschroder TGI 5/100N ignition transformer. An ionization detector is used to detect the flame. The Kromschroder IFS 110IM 10/2/2 automatic controller controls two normally closed solenoid valves, the ignition transformer and the ionization detector. The air supply uses an ASCO Red-Hat solenoid valve, which can operate under a pressure differential of up to 862 kPa. The natural gas line uses an ASCO Red-Hat combustion valve, which can operate under a pressure difference of up to 34.5 kPa, or a capacity of 69.9 kW. The controller will continuously attempt to ignite the flammable mixture until a flame is detected. If the ionization detector does not detect a flame after 10 seconds, the solenoid valves are de-energized, shutting off the flow of natural gas and the air supply solenoid valve. A 3.5-cm-diameter silicon carbide burner tube is used to shape the flame. The ignited gas mixture exits the burner tube at a linear rate of about 15 m/s estimated by the manufacturer. When the mixture enters the larger 15.2-cm-diameter combustion reactor chamber, the velocity is reduced to 3.69 m/s.

3.3.3 Natural gas line and air supply

Natural gas is available in the laboratory at 186 kPa. This pressure is much higher than the desired operating conditions, so the pressure is reduced from supply pressure to the appropriate operation pressure, 1.0~3.0 kPa, by a regulator. After this regulator, a gas flow meter and a mass flow controller are attached. Finally, the above mentioned solenoid valve is installed upstream of the gas burner to turn on/off the gas.

The arrangement of the air supply is similar to that of the gas line. There is only one regulator, as the solenoid valve can handle an inlet pressure of up to 862 kPa. The regulator can reduce the pressure from the compressed-air pressure of 669 kPa to as low as 13.8 kPa, or it can stop the flow of air completely. After this regulator there are an air flow meter and a mass flow controller. The air supply solenoid valve is closed when the burner is not operational, but the operator will want to send air into the reactor as an effort to cool the burner housing, so the air solenoid is by-passed by a ball valve normally open.

3.3.4 Combustion chamber sections

The modular combustion chamber, fabricated by Technical Services, Inc., is made of different-sized sections of 0.953-cm-thick carbon steel. Refer to Reference 26 for the drawings of the individual sections.

The inner diameter of the steel shell is 61.0 cm and there are 71.7-cm flanges welded to each vertical section. The insulation is a layer of Greenlite Express-30 insulation ceramic, an alumina/silica-based material that is mixed like cement and poured around a form. The material contains about 0.7% alkalis, 58.1% alumina, 1% iron oxide, 3.1% lime, 0.2% magnesia, 35.3% silica, and 1.6% titania. The composition of the refractory materials may be significant because refractory materials are reported to cause catalytic oxidation of elemental Hg in combustion tests. The ceramic insulation is anchored to the steel shell by stainless steel anchors welded on the inside shell. Developing an appropriate temperature profile within the reactor was the primary design consideration in its construction. Refer to Reference 26 for detailed discussion.

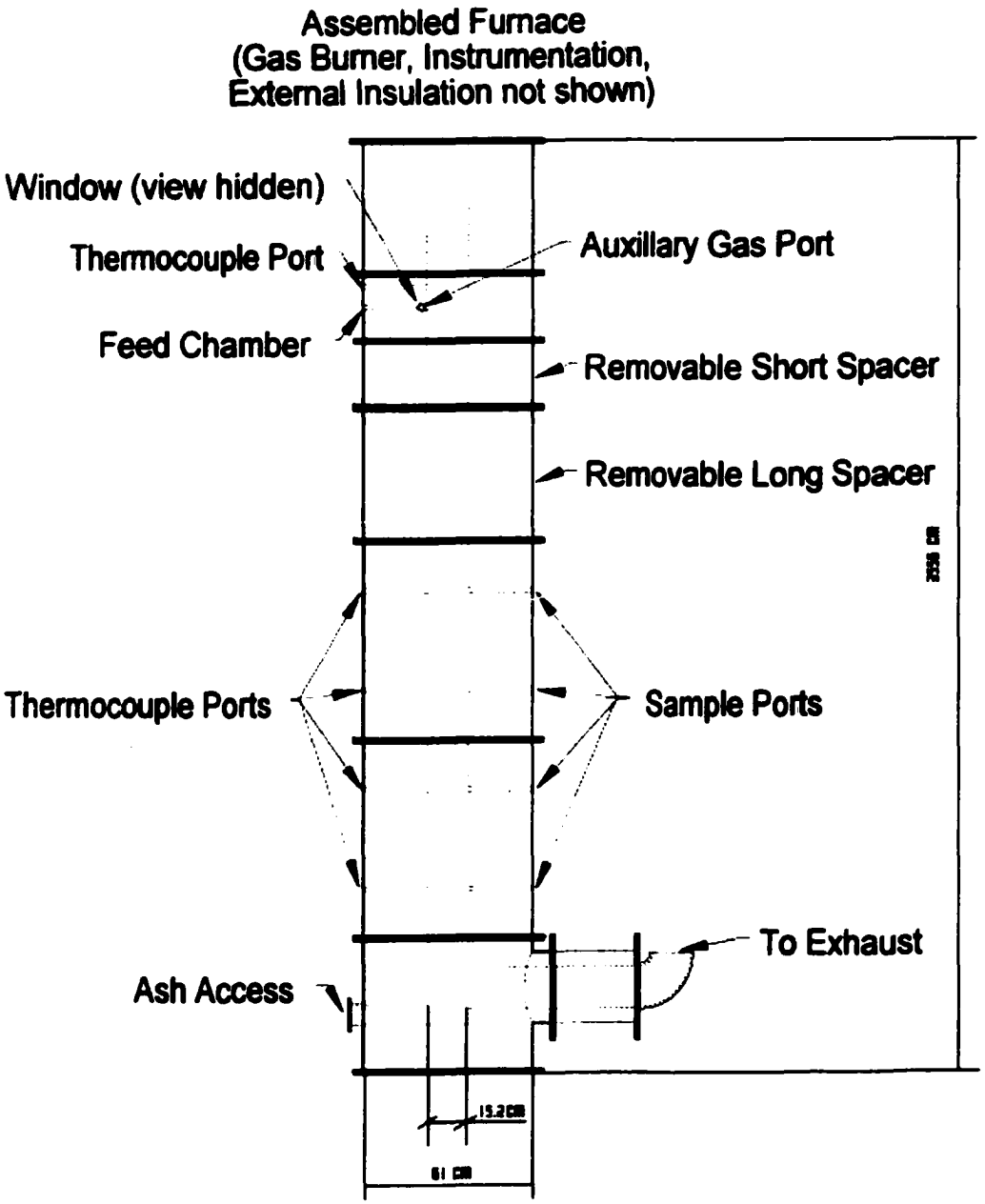

Figure 3. Schematic of the laboratory-scale down-flow combustion reactor

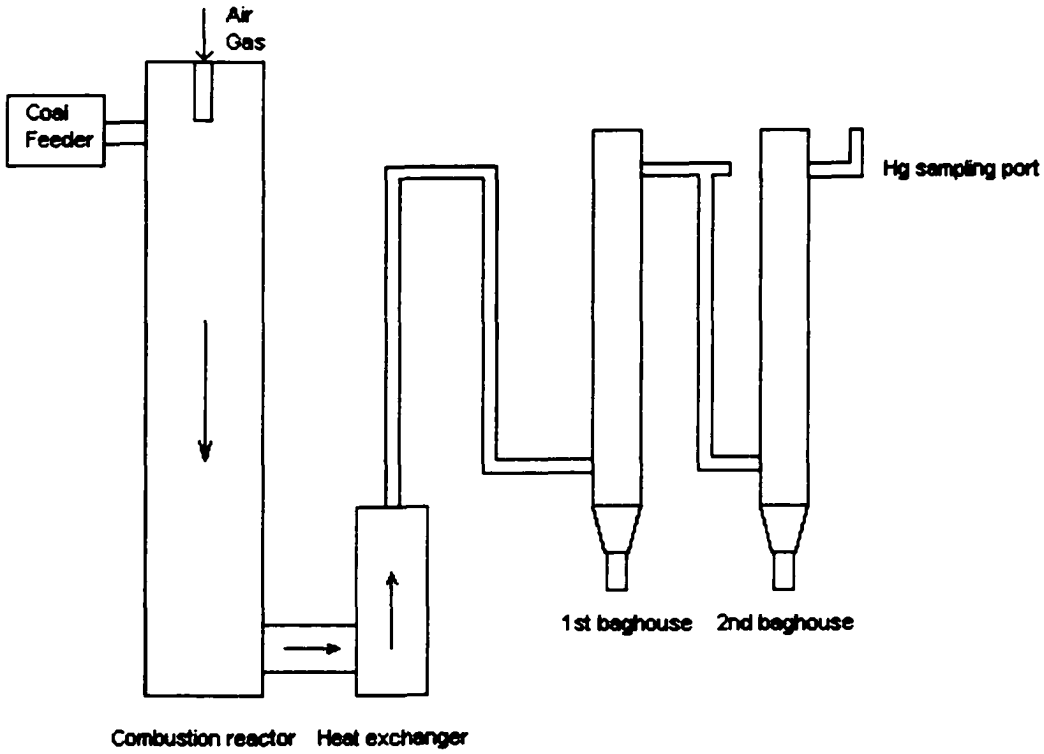

Figure 4. Layout of the laboratory-scale system

The first section is 50.8-cm high. The natural gas burner is attached to the top of the section, and the 30.5-cm-long burner tube extends into this section. The burner is secured to the top of the reactor.

The second section is a 25.4-cm-high feeding zone. The feeding zone has a total of four ports, one for measuring the temperature, one for injecting the fuel, one serves as a window port, and one allows for auxiliary fuel injection. The ports for the thermocouples and the auxiliary gas injection consist of 1.27-cm NPT couplings that are welded to the outside of the steel shell, allowing for the thermocouples to be screwed into place. The window port consists of a 5.08-cm-diameter schedule 40 pipe welded to the outside of the steel shell. A ball valve connected to a union with a watch glass in the middle of the union is attached to provide a window to view the inside of the injection zone. The fuel injection port is a 5.08-cm schedule 40 pipe welded to the outside of the steel shell. A flange is welded to the other side of this short pipe. Different feeding systems can be attached to the flange of the coal injection port.

The third section is 25.4-cm high. The fourth section is 50.8-cm high. These two sections are intended for controlling the chamber height and consequently controlling the residence time and/or the temperature profile of this combustion reactor.

The fifth and sixth are each 76.2-cm high. These sections are the sampling zones. Every 38.1 cm there is sampling zone. Each sampling zone consists of two ports, both with 1.27-cm NPT coupling welded on the outside of the steel shell; one port for measuring the temperature and the other for sampling flue gas.

The bottom section is 50.8-cm high. There are two ports in this section, a port to access any ash that may be collected during normal operation of the reactor, and a larger port

opposite the ash access that leads to the heat exchanger to cool the flue gas. The ash access port is 7.62-cm in diameter, large enough to insert a hose to vacuum out the residual ash.

The heat exchanger, which stands on a T-shaped section of pipe lined with ceramic, consists of an inner pipe and an outer pipe. It cools flue gas to a temperature that the next stage equipment/apparatus can handle. Water is introduced into the space between the inner pipe and the outer pipe. Water flows upward co-currently with flue gas, if there is boiling of water inside, the bubbles will be carried out without accumulating inside the heat exchanger and consequently reducing the performance of the heat exchanger.

There are 5 high-temperature thermocouples installed on the combustion reactor. These five locations are shown in Figure 3. Type R thermocouples made of pure platinum and a platinum/rhodium alloy are chosen. They are contained in alumina thermowells, and extend into the reactor chamber approximately 5 cm. Signals from these thermocouples are fed to the data acquisition system. To perform chemical analysis of the gas stream, gas samples are drawn from sampling ports. Their locations are shown in Figure 3. The gas is filtered of water and particulates before entering the chemical analysis system.

O_2 is measured with a Model 100F galvanic fuel cell oxygen analyzer from California Analytical Instruments, Inc.. NO, NO_2 and total NO_x are measured with a Model 42C high-level chemiluminescence NO-NO_2-NO_x Analyzer from Thermo Environmental Instruments, Inc.. CO and CO_2 are measured with a Model ZRH Infrared Analyzer from California Analytical Instruments, Inc.. SO_2 is measured with a VIA-500 Infrared Analyzer from Horiba.

Signals from these analyzers are fed into the same data acquisition system. The data acquisition system consists of National Instrument hardware and software running on a PC.

3.3.5 Operation of the down-flow combustion reactor

This laboratory-scale combustion reactor is operated on a noncontinuous basis, although continuous running is possible. In order to make the batch operation of this combustion reactor repeatable and efficient, several important parameters need to be under control: temperature profile, fuel feeding rate, fuel-air ratio and residence time. For burning pulverized coal, 2~3 days of precombustion of natural gas is necessary to heat up the combustion reactor to achieve heat equilibrium.

3.3.6 Design of the baghouse

Fabric filters remove dust from a gas stream by passing the stream through a porous fabric. Dust particles form a more or less porous cake on the surface of the fabric. It is normally this cake that actually does the filtration [29].

The manner in which the dust is removed from the fabric is a crucial factor in the performance of the fabric filter system. If the dust cake is not adequately removed, the pressure drop across the system will increase to an excessive amount. If too much of the cake is removed, excessive dust leakage will occur while fresh cake develops. The selection of design parameters is crucial to the optimum performance of a fabric filter system.

Fabric filter systems are frequently referred to as baghouses, since the fabric is usually configured in cylindrical bags. Two common baghouse designs are reverse-air cleaning and pulse cleaning. Baghouses are generally considered to be a superior choice, relative to ESP for fine-particulate control.

Pulse baghouses are designed with internal frame structures, cages, inside the bag to keep it from collapsing. The usual configuration has the cage closed at the bottom and open at the top. In the normal mode of operation, dirty gas enters the housing, heavier particulate

drops out and lighter particulate carries on in the air stream and proceeds to the bag filter. The dust is collected on the outside of the bag, cleaned gas exits through the top opening of the bags. The dust cake is periodically removed by introducing a momentary jet of compressed air (60-120 psi) into the bag causing a sudden bag expansion. A venturi or diffuser helps the even distribution of the inertial force to remove the dust. This bag cleaning technique is quite effective; however, the strength of the air pulse and the frequent bag-to-cage fit tend to limit bag life and increase dust migration through the fabric, thus decreasing dust collection efficiency. The following factors are important to the design and the operation of a pulse baghouse.

- The location of the pulse nozzle must be considered.
- Bag material should be appropriate.
- A large housing volume.
- The pulse duration and intensity should be considered.
- Noncontaminated air must be used.

The selection of the fiber material and fabric construction is important to baghouse performance. The fiber material must have adequate strength at the maximum gas temperature expected and adequate chemical compatibility with both the gas and the collected dust. During the operation of filters, the fabric is covered with a dust cake and the cake thickness continuously varies. Once the dust cake has reformed after each cleaning, sieving is probably the dominant mechanism.

Two important parameters are used to characterize the filtration: Gas-to-cloth ratio, G/C, and pressure drop, ΔP. G/C is a measure of the amount of gas flowing through unit

area of fabric in the baghouse, and is given in terms of the number of cubic meter of gas per minute passing through one square meter of cloth.

$$G/C = \frac{V}{S}$$

where: V = volumetric flow rate of gas, m^3/s

S = the fabric area that gas approaches, m^2

G/C has a unit of linear velocity and thus can be considered a superficial gas velocity. As the gas-to-cloth ratio increases, pressure drop ΔP also increases. Pressure drop here indicates energy loss through a fabric filter. It can be quantitatively described by the following equation describing the pressure drop across a fabric filter with dust cake accumulating on the fabric, which was derived from the basic Darcy equation:

$$\Delta P = S_E V + K_2 C_i V^2 t$$

where: ΔP = pressure drop, N/m^2

S_E = effective residual drag, $N \cdot s/m^3$

V = velocity, m/s

K_2 = specific cake coefficient

C_i = inlet dust concentration, g/m^3

Δt = filtration time, s

Several assumptions are included: the fluid is essentially incompressible and steady, the fluid viscosity is Newtonian, and the velocity is low enough that only viscous effects occur. Filter bags normally have diameters about 14 cm. A G/C of 5 is typically used in fly ash industry. The pulse duration is about 0.1 second if 100-psi compressed air were used.

The baghouses used in this study are commercial products from Staclean Diffuser Company. Staclean dust collectors are state of the art. Cleaning efficiency is 99.9% on all particulate ½ micron and larger in size [30]. The model number is Staclean 1-7-ILF with one filter bag installed. Designed gas flow rate is 1.7 m^3/min. The filter material area is 1 m^2. The designed gas to cloth ratio is 1.7 m/min. The metal housing is made of 25.4-cm mild steel pipe with 10-gauge mild steel tubesheet. The can velocity is 51.2 m/min. Approximate dead load is 77.2 kg. The filter bag and clean gas plenum are accessed from the top of the baghouse. Staclean diffuser is made of galvanized steel. Filter bag is designed with a snapband feature and made of 100% GORE-TEX membrane. Cages are made of galvanized steel, 10 vertical wires, 20.3-cm horizontal ring spacing. The control instrumentation includes a 3010 series photohelic pressure switch/gage in conjunction with a DNC-T 2003 solid-state timer. The compressed air is delivered through a diaphragm pulse valve connected to a 2.54-cm-diameter pipe welded on the top cover. To operate the baghouses, less than 0.059-m^3 compressed air at 550~760 kPa is required. Refer to Appendix 1 for detailed design parameters.

During our testing, the pressure drop across the filter bag is around 498~996 Pa. When the pressure drop exceeds the set point value for a certain amount of time (set on the solid-state timer), the photohelic controller activates the diaphragm pulse valve, an air pulse is released into the cage. The fly ash cake formed on the outside of the filter bag is back flushed and dislodged; thus a cleaning cycle is accomplished.

3.3.7 Fly ash feeder and coal feeding system

Two baghouses are used in the laboratory-scale testing. The first baghouse filters the fly ash of the flue gas emitted from the down-flow combustion reactor firing pulverized coal. Fly ash/fly ash fractions are injected (spiked) into the flue gas at the outlet of the first baghouse. A small volumetric feeder is used to inject fly ash/fly ash fractions derived from full-scale utility boilers firing PRB subbituminous coal and Blacksville bituminous coal. The injection rate can be controlled precisely so that the injected fly ash concentration is close to that of flue gas emitted from the reactor. The gas residence time inside either baghouse is calculated to be roughly 10 seconds.

The effects of the injected fly ash/fly ash fractions on vapor-phase mercury speciation are studied. The fly ash feeder used in this study is an AccuRate 106M volumetric feeder with an adjustable feeding rate of 0.000481~14.15 L/hr. Refer to Appendix 2 for the calibration curves of whole PRB fly ash and whole Blacksville fly ash.

The laboratory-scale testing involves the combustion of pulverized PRB coal and pulverized Blacksville coal. A pneumatic conveying system is utilized. It consists of an AccuRate series 600 volumetric feeder to meter and deliver pulverized coal into a miniature fluidized bed, and a flow rate of 70.8 L/min primary air carries the coal powder through a TYGON tubing to the fuel injection port on combustion chamber feeding zone. The secondary air is delivered vertically downward from the natural gas burner at a flow rate of 600 SLPM.

The primary air conveying coal fuel mixes with secondary air in the feeding zone. The coal is ignited by heat radiation from the high temperature ceramic wall and burns as the

mixed stream flows downward. The flue gas exits the combustion reactor, enters the heat exchanger and then enters the first baghouse.

We had designed a second heat exchanger in an effort to cool the flue gas down to 230 ^{0}C, the temperature that the filter bag can handle without any problem. After building and installing this second heat exchanger, the flue gas temperature dropped to below 100 ^{0}C and consequently flue gas moisture was condensed. The reason turned out to be that the fly ash present in flue gas enhanced the heat exchange coefficient between flue gas and inner wall of the heat exchanger. Some of the fly ash was collected in the conduit upstream of the inlet of the first baghouse. This exchanger was removed and replaced with a section of 5.08-cm pipe.

The purpose of the first baghouse is to retain the fly ash of the flue gas emitted from the reactor. It is not critical to control the temperature inside the first baghouse. The temperature inside the pipe connecting the first and the second baghouses and inside the second baghouse is important since flue gas-Hg-fly ash interactions take place in this environment. The temperature environment is maintained by applying insulation on the first baghouse and the connecting pipe. Heating bands are installed on the second baghouse. This provides a very consistent temperature of about 140 °C between (and including) the exit of the first baghouse and the exit of the second baghouse. The flue gas temperature at the inlet of the first baghouse is controlled at about 230 ^{0}C.

3.3.8 Combustion testing approaches

A typical PRB subbituminous and a typical Blacksville bituminous coal are selected for the laboratory-scale testing. These two types of coals are selected because a high level of

elemental mercury presents in the PRB subbituminous coal combustion flue gas while a high level of oxidized mercury presents in the Blacksville bituminous coal combustion flue gas [1, 9]. Table 2 lists the composition analysis of a typical Pittsburgh bituminous coal, a typical Wyodak subbituminous coal and their flue gases [7].

Table 2. Compositions for a Pittsburgh coal and a Wyodak coal

	Pittsburgh	Wyodak
Ultimate analysis (wt. %)		
H	4.98	7.04
C	76.62	52.84
N	1.48	0.7
S	1.64	0.39
O	8.19	34.54
Ash	7.01	4.49
Minor species in ppmw		
Cl	980	550
Hg	0.11	0.11
Gas composition at SR=1.2 (in vol.%)		
CO_2	14.44	13.86
H_2O	5.69	11.13
O_2	3.86	6.27
N_2	76.59	72.17
Species in ppmv		
SO_2	1166	383
HCl	62	49
Hg	0.00124	0.00172
SO_3	15.5	6.5

These two types of coal are ground and dried. Before each day of testing, the reactor is preheated by burning natural gas for 2~3 days to achieve the desired operating temperature. The pulverized coal to be burned is loaded into an AccuRate 600 series volumetric material feeder. This feeder is calibrated for the coal to be burned. The feeding

rate of coal is determined based on the heat value input into the combustion reactor. The feeding rate of PRB coal is 4.53 kg/hr and that of the Blacksville coal is 4.17 kg/hr. A pneumatic conveying system is connected to the outlet of the coal feeder to transport coal powder to the coal injection nozzle.

The coal is burned inside the down-flow combustion reactor, the fly ash entrained in the flue gas passes through the heat exchanger, a section of direct pipe and then enters the first baghouse. The first baghouse filters the fly ash of the flue gas. The flue gas free of fly ash coming out of the outlet of the first baghouse is spiked with a fly ash derived from the same coal being burned or from a different type of coal. The spiked flue gas flows through the connecting pipe and enters the second baghouse. The spiked fly ash is captured by the second baghouse. The sampling of flue gas for mercury speciation is performed at the exit of the second baghouse. Ontario-Hydro sampling method is used. The sampling line is heated to 150 ^{0}C to enhance the transport of the oxidized mercury. Each sampling is performed for about 75 minutes and tests are performed in duplicate.

The injection nozzle injects pulverized coal through the fuel injection port into the combustion reactor. There was no difficulty performing testing with burning PRB coal. For testing with Blacksville coal, injector was clogged after burning this coal for about 15 minutes. The nozzle extends into the injection port of a depth of about 15 cm. The nozzle is probably heated to a temperature high enough to soften the Blacksville coal powder thus causes the plugging of the injector. Further testing with the Blacksville coal is abandoned.

CHAPTER 4. RESULTS AND DISCUSSION

4.1 Bench-Scale Testing

4.1.1 Preliminary testing

Before commencing the test program, initial tests are performed to obtain preliminary knowledge of the interactions between fly ash and mercury under different conditions. Table 1 lists the individual gas concentrations used in preliminary testing. The concentrations are chosen to simulate the composition of a typical coal combustion flue gas. In this study, individual gas components are either present or not present (on or off) in the final simulated flue gas. Intermediate concentrations are not used.

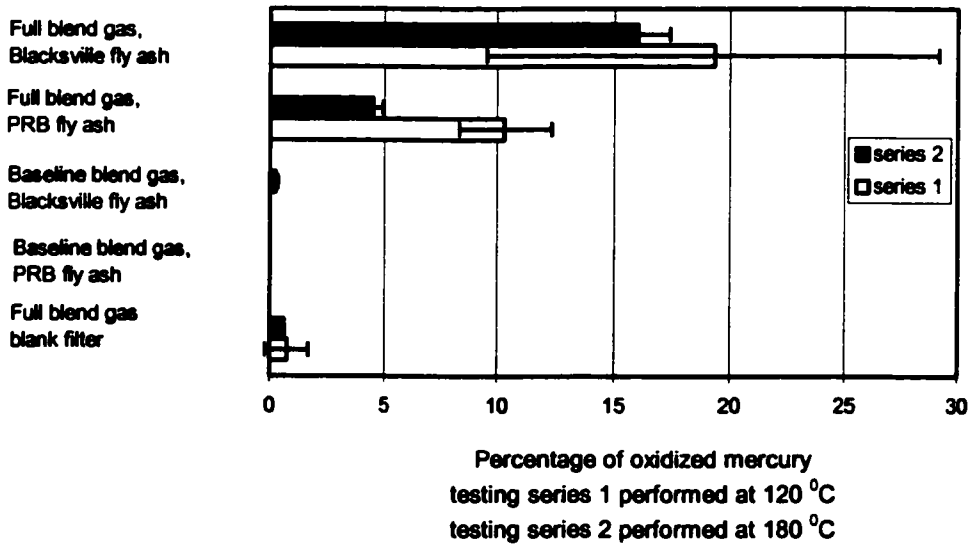

Figure 5. Results of preliminary testing with fly ashes at 120 ^{0}C and 180 ^{0}C

Figure 5 shows the mercury speciation data from the preliminary testing. Each bar represents the average of two duplicated tests. There is almost no Hg^0 transformation detected in tests using baseline simulated flue gas with or without fly ash present. With full blend gas mixture and absence of fly ash, less than 1% of oxidized mercury is detected. This small amount of mercury oxidation is a result of homogeneous gas-phase reactions, or the bench-scale system wall-effect that oxidizes and retains some mercury. With whole Blacksville fly ash presence, oxidized mercury concentrations are higher than those from testing with whole PRB fly ash. Comparing the results from testing at 120 ^{0}C and 180 ^{0}C indicates that the temperature does not appear to have a significant effect on mercury oxidation.

In order to see if the fly ash reactivity changes during the 75 minutes required for a normal sampling, some back-to-back 30-minute testing with the same loaded filters are performed. The results indicate that fly ash reactivity does not change during a normal testing period.

Earlier studies suggested that fly ash derived from bituminous coal and fly ash derived from subbituminous coal are much different with regard to concentrations of TOC, minerals, sulfur compounds and chlorine species [10]. Coals are classified according to their degree of metamorphism. High sulfur bituminous coals typically have high iron content in the form of iron pyrite (FeS_2). It has been observed in the field that bituminous coals with either low or high sulfur contents generally produce a significantly higher emission of oxidized mercury than that produced by subbituminous coals and lignites. The higher chlorine content of bituminous coals is thought to contribute to the formation of oxidized mercury [11].

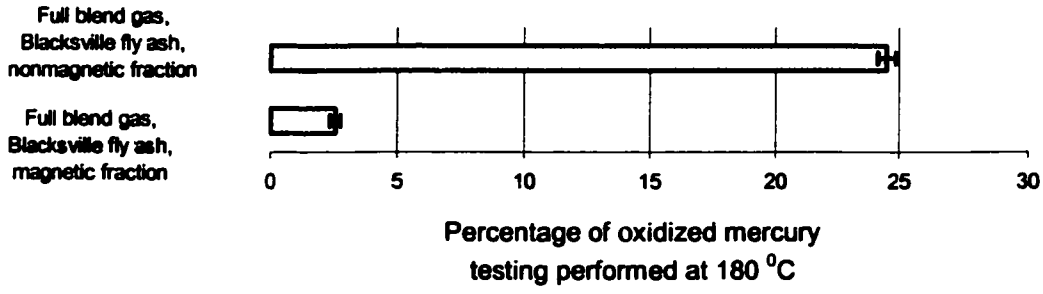

Figure 6. Results of testing with Blacksville fly ash magnetic and nonmagnetic fractions

Blacksville fly ash magnetic and nonmagnetic fractions are separated for further testing. Results are presented in Figure 6. Surprisingly, only 3% of the mercury is oxidized when Blacksville fly ash magnetic fraction is exposed to full blend gas stream at 180 ^{0}C. By comparison, 24% of the mercury is oxidized when testing with Blacksville fly ash nonmagnetic fraction under identical conditions. The iron-rich Blacksville fly ash magnetic fraction does not appear to have a strong catalytic effect on mercury oxidation in these tests. Other researchers [12] have found similar results: "the iron content may not be the important parameter determining the mercury oxidation reactivity."

Figure 7 shows results of full factorial design testing with whole Blacksville fly ash at 180 ^{0}C. No obvious trend is found in the testing. When NO_2 alone or HCl alone is added to the baseline blend, the amount of Hg^0 that is oxidized is much lower than the amount that is oxidized when both NO_2 and HCl are added to the baseline blend. This is called the synergistic effect of NO_2 and HCl. Other researchers also reported this effect [3].

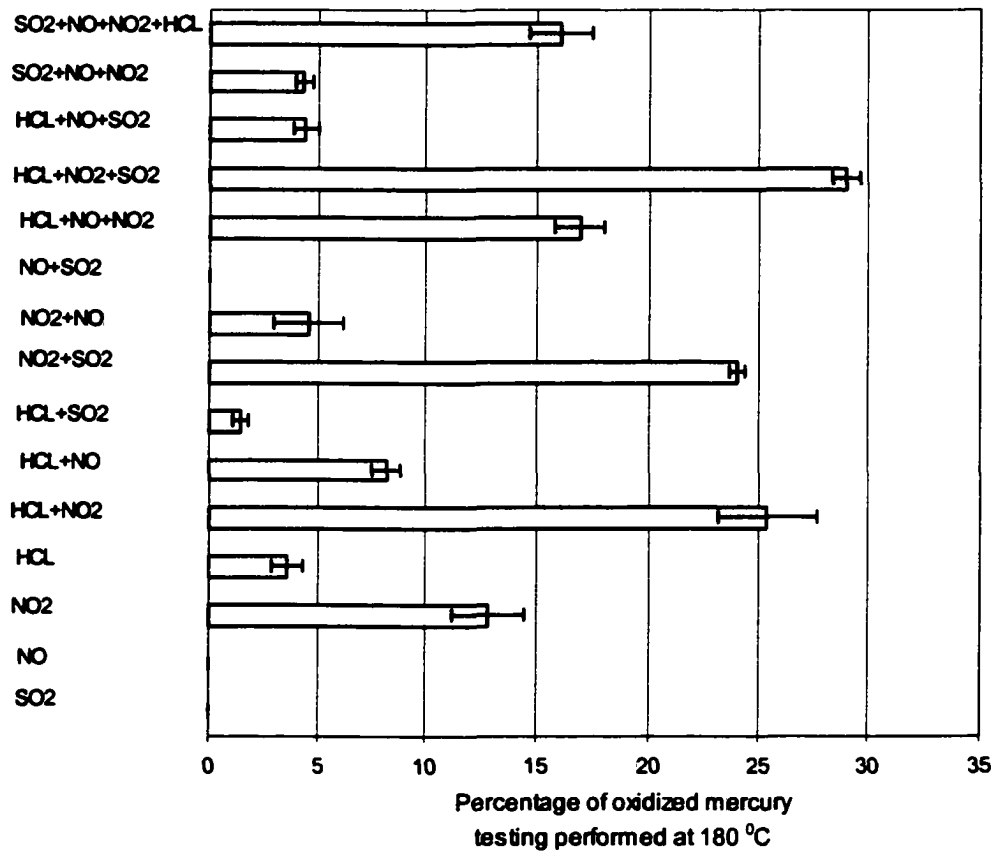

Figure 7. Results of full factorial testing with Blacksville fly ash
(Gases are added to the baseline blend to achieve different gas compositions)

A statistical analysis is applied to the results of the full factorial design testing to determine the effects of individual gas components or gas matrices on mercury oxidation. Pareto chart is used as a representation of the effects. The greater the effects, the farther the bars extend.

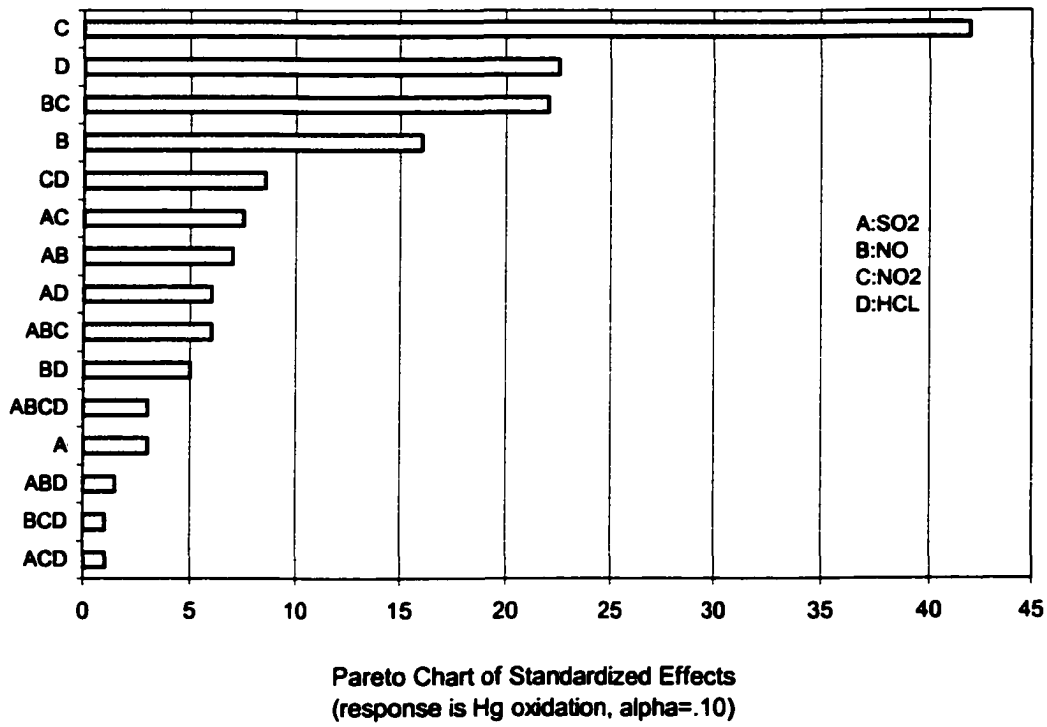

Figure 8. Statistical analysis of the full factorial design testing

Figure 8 shows the standard effects of different gases on mercury oxidation. From this analysis, we draw the following preliminary conclusions:

- The most important factor is NO_2;
- The next are HCl and NO, but the effect of NO depends on NO_2;
- The system is extremely complex.

These conclusions are not surprising considering eight gas components are present and the very complex mineralogy and morphology associated with the fly ash samples used in these tests. In order to further investigate the effects of fly ash on mercury transformation, various techniques are applied to characterize the fly ash samples. Whole fly ashes, sized fly ash fractions and magnetically separated fly ash fractions are characterized.

4.1.2 Effects of gas components

Figure 9 and Figure 10 show the effects of adding NO or HCl to other gases on mercury oxidation. The data are extracted from full factorial testing results. The listed gases are added to the baseline blend. Figure 9 presents the mercury speciation data from testing with whole Blacksville fly ash at 180 ^{0}C with or without NO present. Everything else being equal, the presence of NO appears to inhibit mercury oxidation in four out of the six tests. Other researchers proposed that the large surface area of carbon effectively catalyzes the oxidation of NO to NO_2 at low temperature [14]. In our study the NO inhibiting effect might be the result of competing surface adsorption of Hg^0 and NO so that less Hg^0 is oxidized.

Figure 10 compares mercury speciation data from testing with whole Blacksville fly ash with and without HCl presence. The presence of HCl appears to promote the heterogeneous oxidation of mercury for all gas matrices. Another recent study [13] indicates Cl-atom derived from HCl is responsible for oxidizing Hg^0 via the following important paths:

$$Hg + Cl \leftrightarrow HgCl \qquad (4\text{-}1)$$

$$HgCl + Cl \leftrightarrow HgCl_2 \qquad (4\text{-}2)$$

Mercury oxidation testing over the Blacksville fly ash with high iron content and a subbituminous fly ash with low iron content are conducted in the presence of more complex simulated flue gas by Lee et al.. Their results suggest the strong combined inhibition effect of SO_2 and H_2O on Hg^0 oxidation.

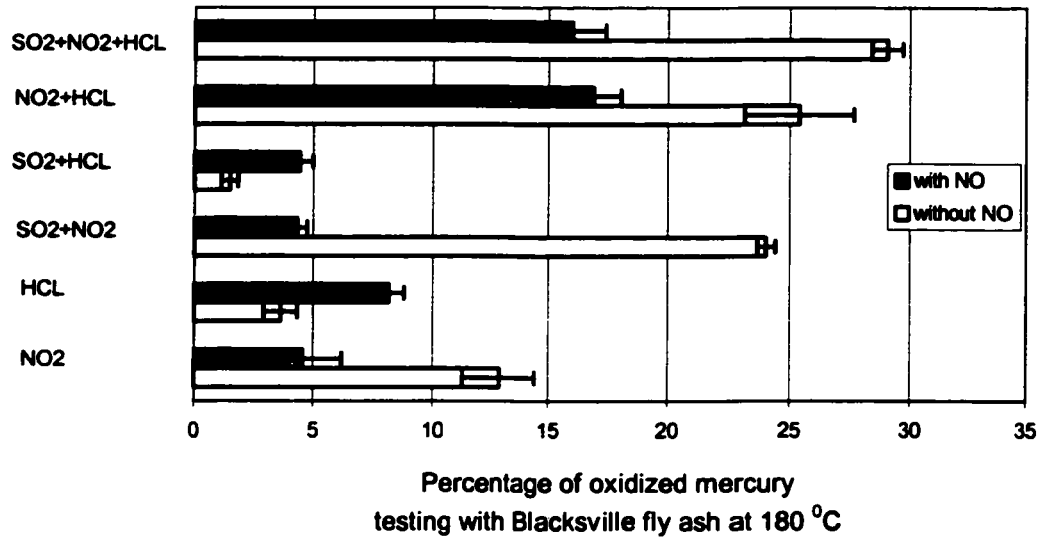

Figure 9. Effects of NO added to gases on mercury oxidation
(Gases are added to the baseline blend to achieve different gas compositions)

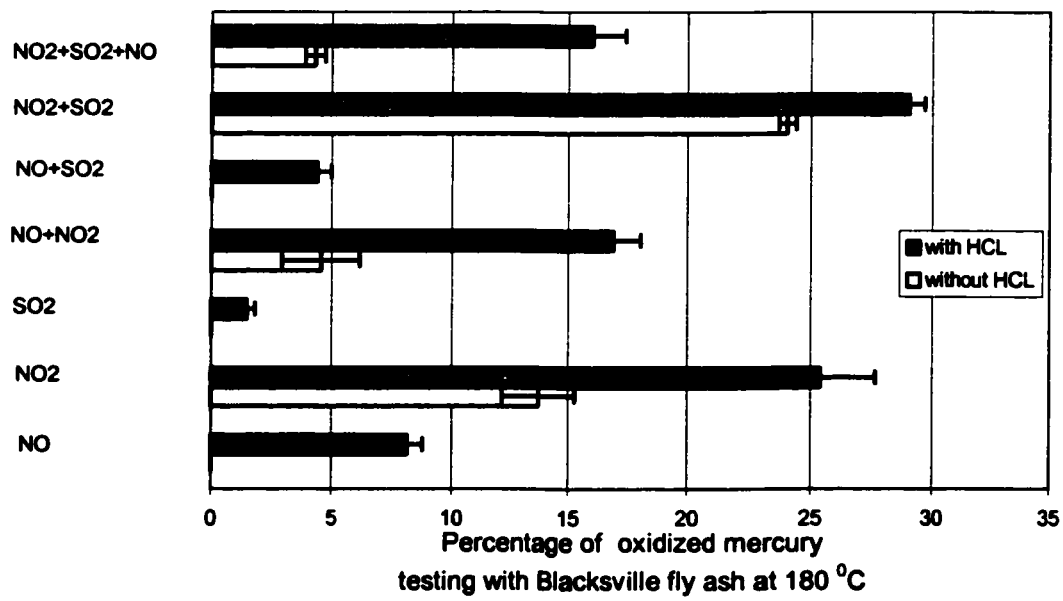

Figure 10. Effects of HCl added to gases on mercury oxidation
(Gases are added to the baseline blend to achieve different gas compositions)

4.1.3 Characterizing fly ash samples

Fly ash samples are characterized using various methods. Sized Blacksville fly ash from cyclone 1 contains magnetic components and nonmagnetic components. All other sized fly ash samples consist of all nonmagnetic material.

SEM analysis of Blacksville fly ash fractions clearly shows the size differences among the fly ash fractions. PRB fly ash fractions also show similar differences. Figure 11 shows the SEM analysis results. These results demonstrate that the cyclone system used in this study effectively sizes the fly ash samples.

The samples have the typical fly ash morphology and consist predominantly of spherical particles. However, for the ash collected in the first cyclone, the Blacksville fly ash is substantially less homogenous and contains more porous and irregularly shaped particles than the PRB fly ash. Differences between the two fly ash samples are less pronounced for the catches from the second cyclone.

Figure 12 shows the results of SEM-EDX analysis of the fly ash samples. The SEM-EDX analysis of the Blacksville fly ash indicates that the highly magnetic fraction in the first cyclone catch contains roughly 26%(atomic) Fe, about 8% Al, about 13%Si, 2% Ca, and lesser amounts of Na, S, K, and Ti. The magnetic fraction has a significant amount of Al and Si. Significant amounts of Fe are typically dissolved (atomic substitutions) in a glass aluminosilicate matrix. The nonmagnetic Blacksville fly ash fraction in the first cyclone catch contains only about 4% (atomic) Fe, 11% Al and 19% Si. The nonmagnetic ash fraction also contains about 2% Ca with lesser amounts of Na, Si, K, and Ti. The chemical composition of the Blacksville fly ash from the second cyclone catch is all nonmagnetic and very similar to the chemical composition of the nonmagnetic ash from the first cyclone catch.

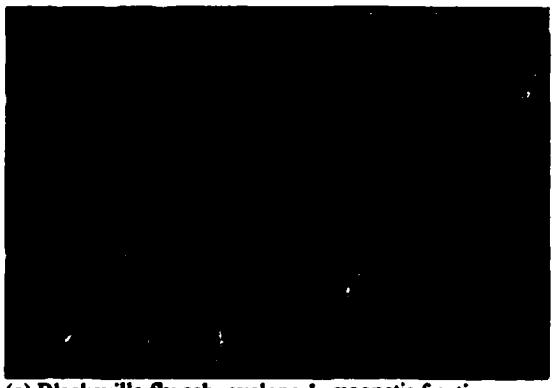

(a) Blacksville fly ash, cyclone 1, magnetic fraction

(b) Blacksville fly ash, cyclone 1, nonmagnetic fraction

(c) Blacksville fly ash, cyclone 2, all nonmagnetic fraction

(d) PRB fly ash, cyclone 1, all nonmagnetic

(e) PRB fly ash, cyclone 2, all nonmagnetic

(f) PRB fly ash, cyclone 3, all nonmagnetic

Figure 11. SEM analyses of fly ash samples

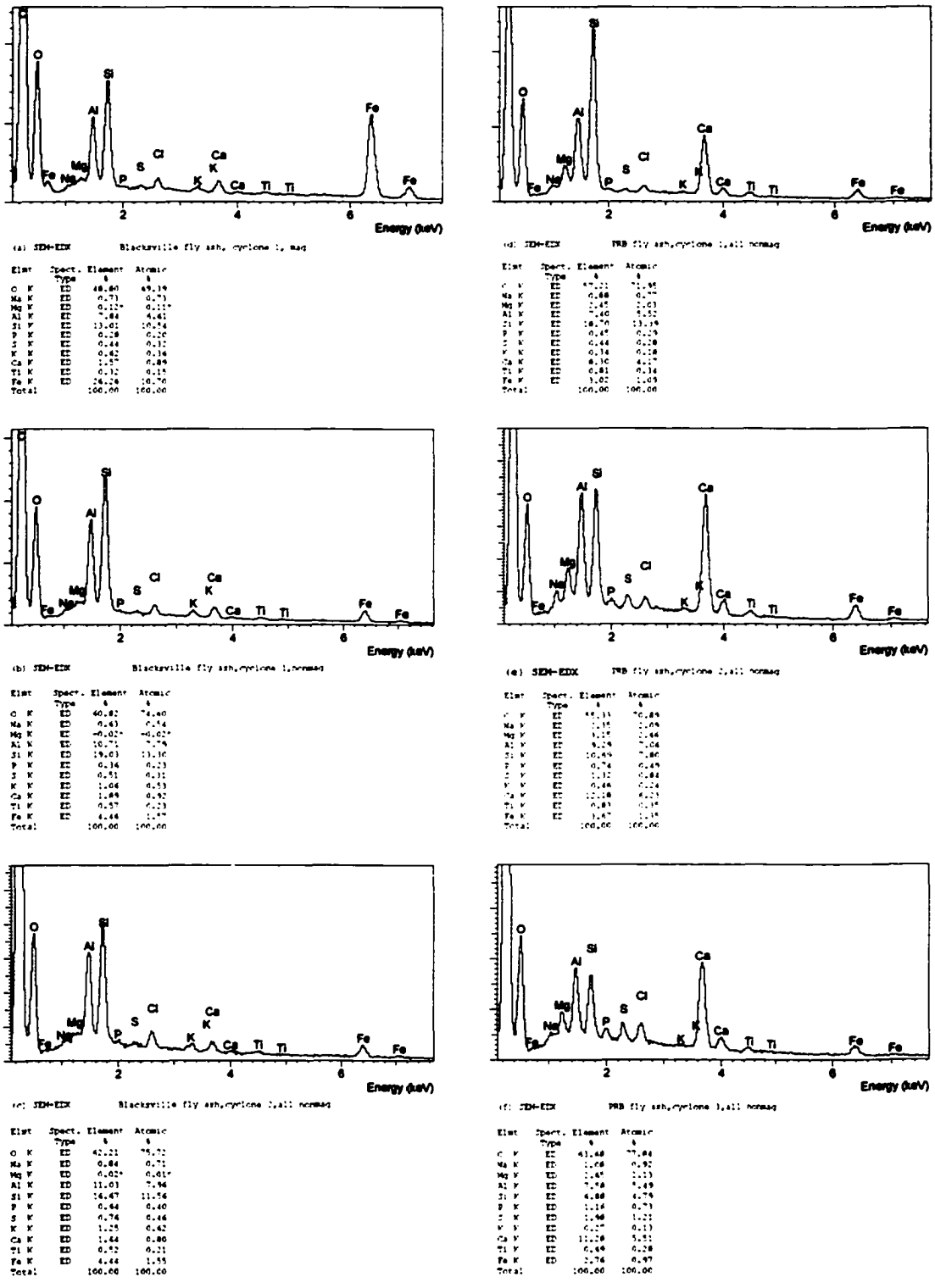

Figure 12. SEM-EDX analyses of fly ash samples

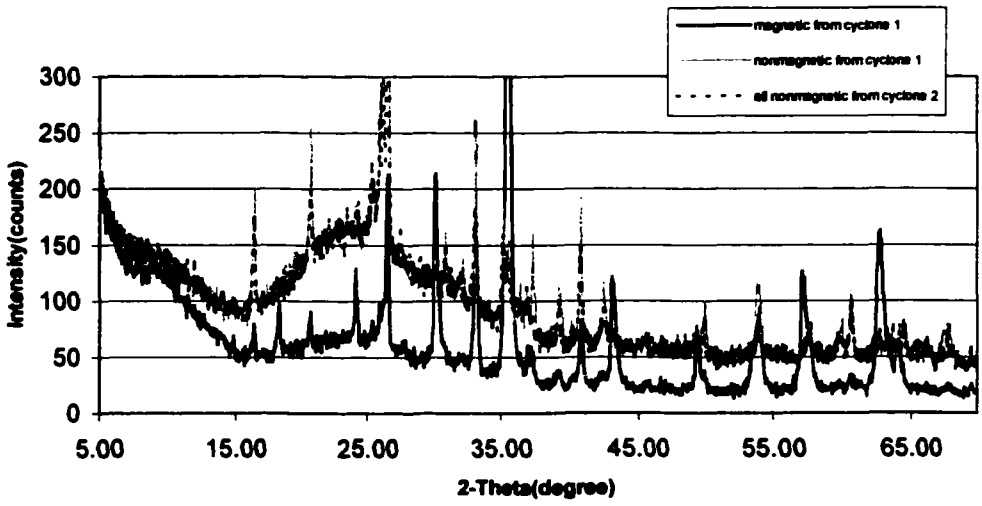

(a) Blacksville fly ash samples

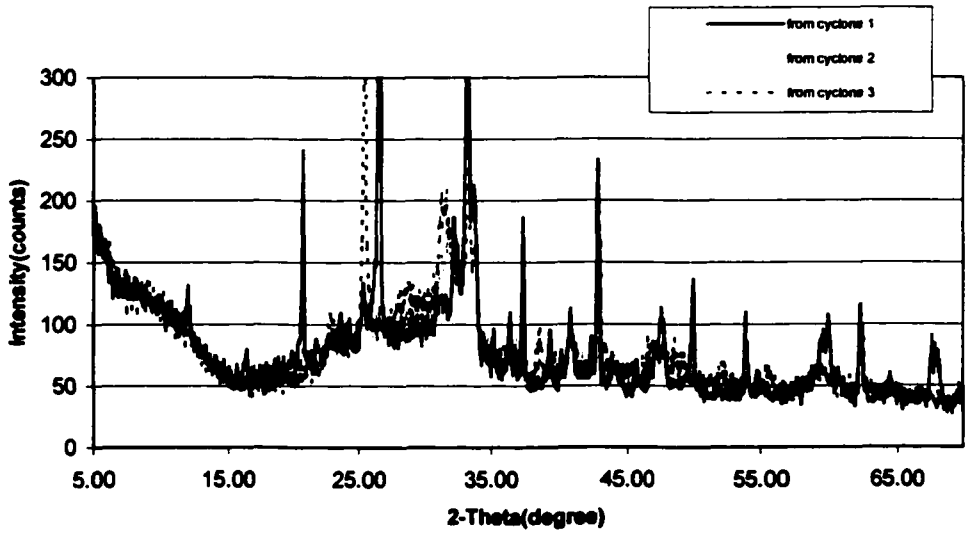

(b) PRB fly ash samples

Figure 13. XRD analyses of Blacksville fly ash and PRB fly ash samples

For the PRB fly ash (all nonmagnetic), the catches from the first and second cyclones contain about 3% (atomic) Fe, 10-20% Al and Si, about 10% Ca, and 2% or less amount of Mg, S, K, and Ti. The first cyclone catch is enriched in Si relative to Al, while the second cyclone catch contains similar amounts of Si and Al.

XRD identifies the crystalline constituents of a sample. The XRD results indicate that the whole Blacksville fly ash consists primarily of quartz (SiO_2), mullite ($Al_6Si_2O_{13}$), magnetite (Fe_3O_4), hematite (Fe_2O_3) and a small amount of lime (CaO). As expected, there is a clear enrichment of the iron oxides relative to the quartz and mullite phases in the magnetic fly ash fraction from the cyclone 1 catch. The nonmagnetic fraction from cyclone 1 is enriched in quartz and mullite relative to the iron oxides. The sized Blacksville fly ash from the second cyclone catch is nonmagnetic, and its composition is very similar to the mineralogical composition of the nonmagnetic ash from the first cyclone. A substantial amount of noncrystalline material is evident in the ash collected from the second cyclone and the nonmagnetic fraction from first cyclone. Figure 13 (a) clearly shows the differences of constituents among the Blacksville fly ash samples.

The PRB fly ash consists primarily of quartz with lesser amounts of lime, periclase (MgO) and calcium aluminum oxide ($Ca_3Al_2O_6$). No magnetic or hematite phases are detected. The sized PRB fly ash fractions in the 3 cyclones are all nonmagnetic and very similar in composition in terms of mineralogy. Figure 13 (b) clearly shows this similarity.

Table 3. BET N_2 isotherm surface area and pore diameter for fly ash samples

Sample ID	Surface Area (m^2/g)			Average Pore Dia. (Å)
	Total	External	Micropore	
Whole Blacksville fly ash	3.4	2.3	1.1	52
Blacksville fly ash, cyclone 1, magnetic	1.5	1.1	0.4	54
Blacksville fly ash, cyclone 1, nonmagnetic	4.8	3.3	1.5	45
Blacksville fly ash, cyclone 2, all nonmagnetic	7.2	5.2	2.0	53
Whole PRB fly ash	1.5	1.0	0.5	57
PRB fly ash, cyclone 1, all nonmagnetic	1.7	1.0	0.7	43
PRB fly ash, cyclone 2, all nonmagnetic	2.0	1.6	0.4	83

The BET surface area (both external and micropores) and average pore diameter are determined for the samples used in this study. Results are shown in Table 3.

The surface area of the whole Blacksville fly ash is significantly higher than that of the whole PRB fly ash. The surface area of the magnetic Blacksville fly ash fraction in the first cyclone is substantially lower than the nonmagnetic fraction in the same cyclone catch. The Blacksville fly ash from the second cyclone catch is substantially higher in surface area than PRB fly ash from the second cyclone catch. For each whole fly ash sample, the BET measurements show that about 70% of the total surface area is external surface area, with the remainder as micropore surface area. The BET average pore diameter is comparable for the whole Blacksville fly ash and whole PRB fly ash. The total surface area, external surface area, and micropore surface area of whole Blacksville fly ash are about twice of those for

whole PRB fly ash. For the samples analyzed, a fraction that has a relatively high total surface area also tends to be high in both the external and micropore surface areas.

Table 4. TOC measurements for fly ash samples

Fly Ash Samples	TOC wt.%
Whole Blacksville fly ash	3.6
Blacksville fly ash, cyclone1, magnetic	0.39
Blacksville fly ash, cyclone1, nonmagnetic	3.9
Blacksville fly ash, cyclone2, all nonmagnetic	0.13
Whole PRB fly ash	0.08
PRB fly ash, cyclone 1, all nonmagnetic	NA
PRB fly ash, cyclone 2, all nonmagnetic	NA

Table 4 shows the TOC of the fly ash samples. The whole Blacksville fly ash has about 3.6% TOC, while whole PRB fly ash contains less than 0.1%. The TOC in the Blacksville fly ash is highly concentrated in the nonmagnetic fraction from the first cyclone catch.

After characterizing fly ash samples, several tests are conducted to determine the effects of iron content, particle size and surface area of fly ash on the oxidation of mercury with simulated flue gas.

4.1.4 Effects of iron content

Figure 14 shows the results of testing with Blacksville fly ash magnetic and nonmagnetic fractions collected from the first cyclone. The tests are performed at 180 ^{0}C with various gases added to the baseline blend.

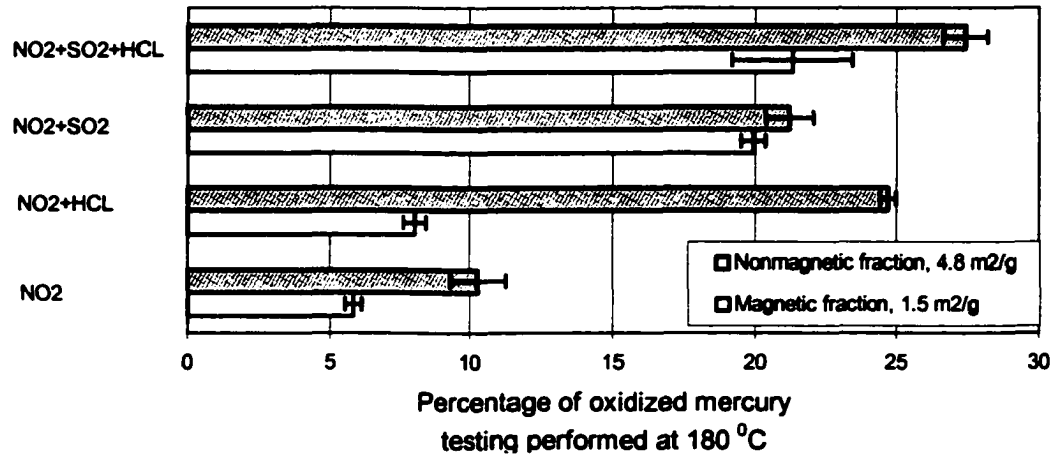

Figure 14. Comparison of the oxidizing reactivity of Blacksville fly ash fractions from cyclone 1, with various gas components added to the baseline blend

It is expected that the magnetic fractions would yield more oxidized mercury because the iron-rich fractions could possibly have a higher catalytic reactivity. However, the nonmagnetic fraction from the first cyclone catch is always more catalytic than the magnetic fraction collected in that cyclone. The difference is significant when NO_2 and HCl are added to the baseline blend.

From these results and the discussion in section 2.4, iron content does not appear to be the primary factor determining the Hg^0 oxidation reactivity of this bituminous coal fly ash. Other physical and chemical properties of the fly ash may also play a role in determining reactivity.

Figure 14 shows that the nonmagnetic fraction with a surface area of 4.8 m^2/g is more effective than the magnetic fraction with a surface area of 1.5 m^2/g. Specific surface area

appears to be important for the heterogeneous conversion of Hg^0 to an oxidized form in this series of tests.

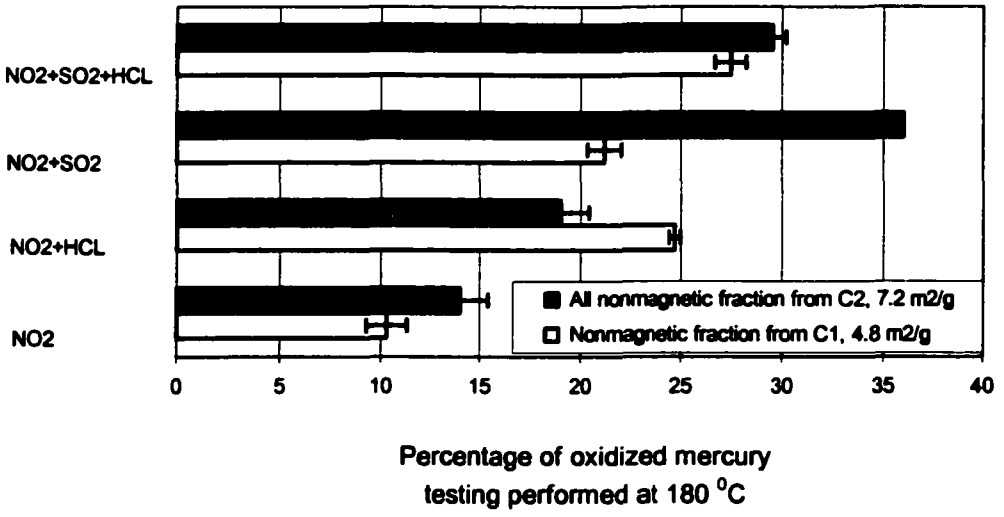

Figure 15. Comparison of the oxidizing reactivity of nonmagnetic Blacksville fly ash fractions from cyclone 1 and cyclone 2

4.1.5 Effects of particulate size and specific surface area

Figure 15 compares the oxidizing reactivity of the two different sized nonmagnetic Blacksville fly ash fractions under various simulated flue gas conditions. In three of the four tests, more mercury oxidation is observed when using the smaller particle size fraction, although the differences are sometimes minimal. A tendency toward greater oxidation with small particles would be expected considering the surface area difference between the two sized fractions. It is not known why that this does not hold true when adding NO_2 and HCl to the baseline blend. It is interesting to note that for both Figures 14 and 15, the data obtained when adding NO_2 and HCl to the baseline blend does not match the trend observed for the

other speciation data within a given series of tests. Further study is needed to explain the effects of adding NO_2 and HCl to baseline blend.

For data presented in Figures 14 and 15, the oxidation of Hg^0 observed in these two series of tests are comparable, even though the fly ash samples used in these two series of tests differ greatly in total organic carbon (3.9% vs. 0.39% and 3.9% vs. 0.13%, respectively). The TOC does not appear to be important for Hg^0 oxidation based on the limited data collected.

Figure 16 shows the results of testing with sized fly ash samples at 180 ^{0}C with NO_2, SO_2, and HCl added to baseline blend.

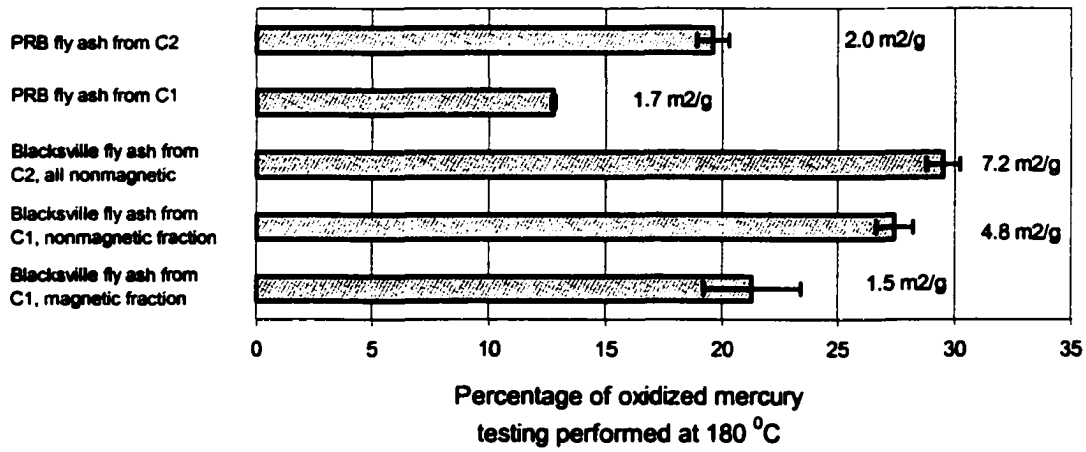

Figure 16. Effects of fly ash on mercury oxidation with NO_2, SO_2 and HCl added to baseline blend

For PRB fly ash fractions, the catch from the second cyclone has a smaller particle size and larger surface area and has a larger catalytic activity for oxidizing Hg^0. For the Blacksville fly ash fractions, the magnetic and nonmagnetic fractions from cyclone 1 have

the same particle size but the magnetic fraction has a smaller surface area. The fly ash fraction with the largest surface area converts the largest amount of Hg^0 to the oxidized form while the fraction with the smallest surface area converts the smallest amount of Hg^0. It is interesting to compare the speciation data for the Blacksville fly ash magnetic fraction from cyclone 1 and the PRB fly ash fraction from cyclone 1 which is nonmagnetic. The two fractions have the same particle sizes and comparable surface areas (1.5 m^2/g vs. 1.7 m^2/g), but the Blacksville fraction converts more Hg^0 than PRB fraction does. The Blacksville fraction has much higher iron content (26%) than the PRB fraction (3%). Iron as a transitional metal reacting as a catalyst might explain this significant difference.

It is interesting to observe the correlation between the percentage of oxidized mercury and the specific surface area of the fly ash samples, as presented in Figure 15. SEM-EDX, XRD and BET N_2 isotherm analyses demonstrate that these fly ash samples (except for Blacksville fly ash magnetic fraction) have similar morphology and mineralogy while having significant differences of surface area. It is obvious that for the four fly ash samples, as the fly ash sample surface area increases, the percentage of oxidized mercury increases. In other words, the surface area of a fly ash sample is very important to the oxidation of mercury under the testing conditions.

4.2 Results From Combustion Testing

Due to problems encountered with burning Blacksville coal, all laboratory-scale testing is performed with burning PRB coal only. Flue gas from burning PRB coal is

analyzed for CO, CO_2, NO, NO_2, O_2 and SO_2 concentrations. Table 5 lists the concentrations of these gases during the combustion of the PRB coal.

Table 5. Compositions of PRB coal combustion flue gas

Gas component	Concentration (Molar)
CO	30 ppm
CO_2	14%
NO	300 ppm
NO_2	< 3 ppm
O_2	6%
SO_2	100 ppm

Table 6. Results of combustion testing with or without fly ash spiking

Testing description	Fly ash injection rate g/min	Oxidized mercury for each test %	Average oxidized mercury %	Total mercury recovery %	Average total mercury recovery %
No ash spiking Day 1 Day 2		 62,71 51,67	63	 36,56 25,36	38
Whole PRB fly ash Day 1 Day 2	7.8	 26,27 9,14	19	 37,17 19,14	22
Whole Blacksville fly ash	7.8	45,56	50	14,25	20
Blacksville fly ash, nonmagnetic fraction	4.1	30,54	42	16,19	18
Blacksville fly ash, magnetic fraction	6.5	32,50	41	17,16	17

There are 14 tests performed with burning PRB coal. Mercury speciation data and recoveries are listed in Table 6. Data presented in a line represent tests in duplicate performed on the same day. The tests performed without spiking fly ash are repeated on a different day. Tests performed with spiking whole PRB fly ash are also repeated.

Data from the testing without spiking fly ash show reasonable repeatability. All other testing show some scattering compared with the data from bench-scale testing.

No analysis is performed to determine the total mercury content of the PRB coal used in the laboratory-scale testing. A value of 80 ppbw is used to estimate the total mercury recovery for all the tests. Based on this literature value, the average total mercury recovery for all the combustion testing is about 23%, assuming all the mercury is released into flue gas during combustion process. This apparently low mercury recovery could be due to several reasons:

- The insulation refractory inside the combustion reactor chamber might catalytically oxidize mercury; thus produces substantial quantities of oxidized mercury in the flue gas. The wall/volume ratio of this combustion reactor is relatively large due to the small size of the combustion reactor, some mercury is probably absorbed by the flue gas conduit, i.e. wall-effect may be important in the laboratory-scale testing.
- Large amount of particulate mercury is produced. The mercury captured by the fly ash retained in the first baghouse represents a significant portion of the total mercury in the PRB coal.
- The highest total mercury recovery is from the testing without fly ash spiking. All other testing with fly ash spiking has lower total mercury recoveries. This indicates the injected fly ash probably adsorbs vapor-phase mercury.

The low mercury recoveries indicate longer pre-combustion time is needed to establish the wall-effect equilibrium before sampling of flue gas is performed. The mercury speciation data indicates the highest amount of oxidized mercury (63%) is obtained from the

testing without fly ash spiking. However, the high percentage of oxidized mercury in flue gas derived from PRB coal is not in agreement with the literature values. This is probably due to the significant wall-effect of the combustion reactor.

Testing with spiking whole PRB fly ash has an oxidized mercury percentage of 19% and total mercury recovery of 22%. Testing with spiking whole Blacksville fly ash has an oxidized mercury percentage of 50% and the total mercury recovery of 20%. Total mercury recoveries from these two tests are comparable. Spiking with whole PRB fly ash yields a much lower percentage of oxidized mercury than that from spiking with whole Blacksville fly ash. This indicates whole Blacksville fly ash is more reactive than whole PRB fly ash.

Testing with spiking nonmagnetic Blacksville fly ash has an oxidized mercury percentage of 42% and a recovery of 18%. Testing with spiking with magnetic Blacksville fly ash has an oxidized mercury percentage of 41% and a recovery of 17%. Both tests have close percentages of oxidized mercury and total mercury recoveries. Substantial differences are not observed between these two testing, even though the two fly ashes have significant difference of specific surface area.

Whole PRB fly ash and whole Blacksville fly ash injection rates are kept the same at 7.8 g/min. Blacksville fly ash magnetic fraction injection rate is 6.5 g/min while nonmagnetic fraction from the same ash is injected at a rate of 4.1 g/min. The nonmagnetic fraction is injected at a lower rate while the two fractions achieve almost the same percentages of oxidized mercury. It appears that nonmagnetic fraction (4.8 m^2/g) has a higher reactivity than magnetic fraction (1.5 m^2/g) to oxidize Hg^0 provided that all the other conditions are the same.

CHAPTER 5. CONCLUSIONS

5.1 Conclusions

The presence of fly ash is a critical factor for the heterogeneous Hg^0 oxidation in bench-scale testing. Fly ash specific surface area has a determining effect on Hg^0 heterogeneous oxidation, provided that the fly ash samples have similar morphology, mineralogy and testing performed in same flue gas matrices. The flue gas components, including NO_2, HCl, NO and SO_2, have strong effects on the potential of whole fly ashes to oxidize Hg^0. Temperature does not appear to have a significant effect on mercury oxidation. Iron content may have effects on Hg^0 oxidation. Although the amount of TOC in fly ash does not show a strong effect on Hg^0 oxidation, Blacksville fly ash has a TOC more than 10 times that of PRB fly ash. This difference could contribute to the different mechanisms involved in the oxidation of Hg^0 by different types of coal fly ash.

Based on the limited number of combustion tests performed and the scattering of the data, fly ash specific surface area appears to be an important factor determining the mercury speciation in coal combustion flue gas. Definitive conclusions cannot be drawn for the laboratory-scale combustion testing about the relative catalytic reactivity of whole fly ashes and fly ash fractions.

5.2 Suggested Future Work

Although the Ontario-Hydro method provides results with a high level of accuracy of mercury speciation and good repeatability, it requires a high level of quality control, well-

trained personnel and provides no real-time data. Automated on-line mercury analyzers need to be developed to measure both mercury speciation and total mercury emissions.

More research is needed to investigate the nature of the surface chemistry involved in Hg^0 heterogeneous oxidation. X-ray Adsorption Fine Structure (XAFS) analysis will help to identify the mercury species adsorbed on the fly ash samples [1,6,15,16]. Special sampling techniques combined with mass spectrometry will identify the Hg species present in the vapor phase and condensed phases, respectively [17]. In-situ studies will help identify the mechanisms responsible for heterogeneous mercury transformations by fly ash [18,19].

Effects of moisture content reported by different researchers appear controversial, more testing needs to be done to investigate the effects of moisture on mercury oxidation during post-combustion conditions. Effects of iron content and TOC need to be explored.

Wall-effect might not be so apparent in a full-scale coal-fired boiler, it causes uncertainties in the laboratory-scale testing results. More combustion testing with PRB subbituminous coal and Blacksville bituminous coal under a variety of conditions needs to be performed in order to fully understand the mercury chemistry during post-combustion conditions.

APPENDIX 1. STACLEAN BAGHOUSE DESIGN PARAMETERS

Model: Staclean 1-7-ILF

CFM: 60 at 220 ^{0}F

Number of filters: 1 bag

Filter media area: 10.77 sq. ft.

G/C ratio: 5.57

Can velocity: 168 fpm

Housing: 10" mild steel pipe

Tubesheet: 10 ga mild steel, 10" diameter

Approximate dead load: 170 lbs

Bag access: top removal

Clean air plenum access: bolt on top

Staclean Diffuser: galvanized

Filter bags: snapband, 100% Teflon with GORE-TEX Membrane

Cages: galvanized steel, 10 vertical wires, 8" horizontal ring spacing

Instrumentation: photohelic

Timer: solid state

Diaphragm valve and blow pipe: 1" diameter

Compressed air requirements: less than 2.1 cu. ft. at 80-110 psi

Discharge: 6 inch

Miscellaneous:

- Solenoid prepiped to the valves
- Tubesheet with perimeter welding
- Conical hopper
- High temperature gasket
- High temperature coupling
- Flanged inlet, outlet and discharge
- Preassembled

APPENDIX 2. THE CALIBRATION CURVES FOR WHOLE PRB AND WHOLE BLACKSVILLE FLY ASHES

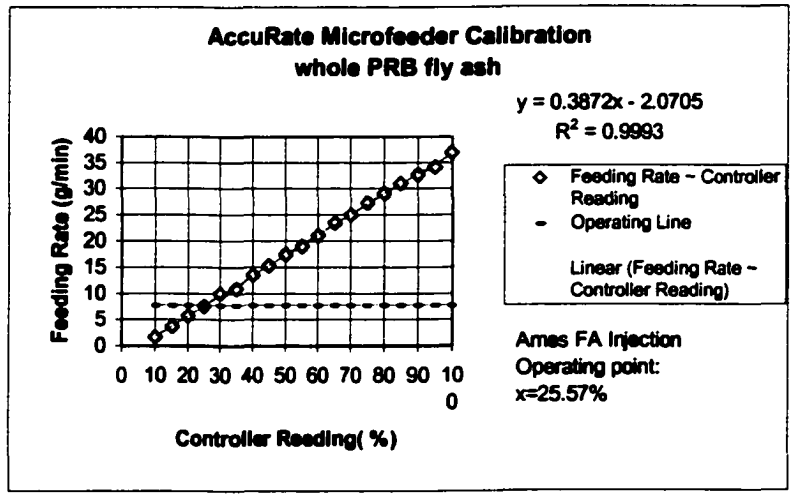

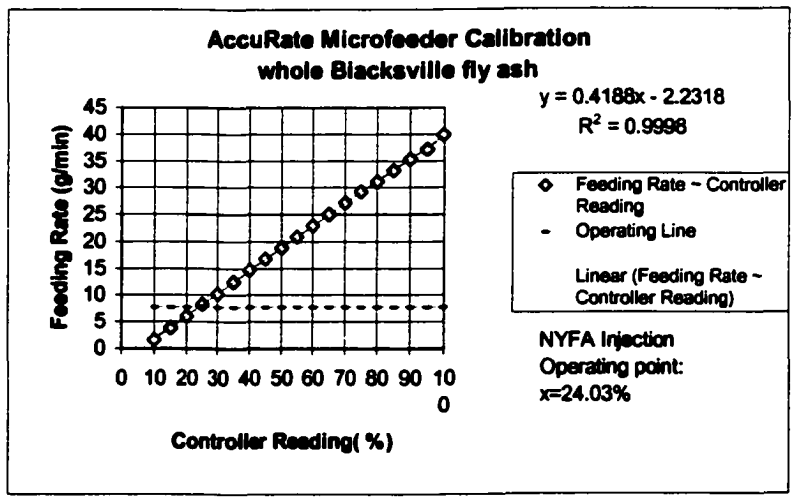

REFERENCES

1. Brown, T.D., Smith, D.N., Hargis, R.A., Jr. and O'Dowd, W. J. "1999 Critical Review." Journal of the Air & Waste Management Association, June, 1999

2. "EPA decides mercury emissions from power plants must be reduced." Environmental Protection Agency, December 14, 2000, http://www.epa.gov/mercury

3. Hall, B., Lindqvist, O. and Ljungstrom, E. "Mercury chemistry in simulated flue gases related to waste incineration conditions." Environmental Science and Technology, 24, 108-111, 1990

4. Hall, B., Schager, P. and Lindqvist, O. "Chemical reactions of mercury in combustion flue gases." Water, Air and Soil Pollution, 56, 3-14, 1991

5. Niksa, S. and Helble, J.J. "Interpreting laboratory test data on homogeneous mercury oxidation in coal-derived exhausts." Proceedings of Air & Waste Management Specialty Conference on Mercury Emissions: Fate, Effects, and Control, Chicago, Illinois, August 21-23, 2001

6. Senior, C.L, Bool, L.E., III, Huffman, G.P., Huggins, F.E., Shah, N., Sarofim, A., Olmez, I. and Zeng, T. "A fundamental study of mercury partitioning in coal fired power plant flue gas." Proceedings of 90th Air & Waste Management Association Annual Meeting, Toronto, Canada, June 8-13, 1997

7. Senior, C.L., Sarofim, A.F., Zeng, T., Helble, J.J. and Mamani-Paco, R. "Gas-phase transformations of mercury in coal-fired power plants." Fuel Processing Technology, 63, 197-213, 2000

8. Edwards, J.R., Srivastava, R.K. and Kilgroe, J.D. "A study of gas-phase mercury speciation using detailed chemical kinetics." Journal of Air & Waste Management Association, 51, 869-877, June, 2001

9. Laudal, D.L., Heidt, M.K., Galbreath, K.C., Nott, B.R. and Brown, T.D. "State of the art: mercury speciation measurement in coal combustion systems." Proceedings of 90th Air & Waste Management Association Annual Meeting, Toronto, Canada, June 8-13, 1997

10. Hower, J.C., Rathbone, R.F., Robertson, J.D., Peterson, G. and Trimble, A.S. "Petrology, mineralogy, and chemistry of magnetically-separated sized fly ash." Fuel, 78, 197-203, 1999

11. Krishnan, S.V., Gullett, B.K. and Jozewicz, W. "Sorption of Elemental Mercury by Activated Carbons." Environmental Science and Technology, 28, 1506-1512, 1994

12. Lee, C.W., Srivastava, R.K., Kilgroe, J.D. and Ghorishi, S.B. "Effects of iron content in coal combustion fly ashes on speciation of mercury." Proceedings of 94th Air & Waste Management Association Annual Meeting, Orlando, Florida, June 24-28, 2001

13. Sliger, R.N., Kramlich, J.C. and Marinov, N.M. "Development of an elementary homogeneous mercury oxidation mechanism." Proceedings of 93rd Air & Waste Management Association Annual Meeting, Salt Lake City, Utah, June 18-22, 2000

14. Mochida, I., Shirahama, N., Kawano, S., Korai, Y., Yasutake, A., Tanoura, M., Fujii, S. and Yoshikawa, M. "NO oxidation over activated carbon fiber (ACF). Part 1. Extended kinetics over a pitch based ACF of very large surface area." Fuel, 79, 1713-1723, 2000

15. Huggins, F.E., Huffman, G.P., Dunham, G.E. and Senior, C.L. "XAFS examination of mercury capture on three activated carbons." ACS Division of Fuel Chemistry Preprints, 42, No. ¾, 1997

16. Huggins, F.E., Yap, N., Huffman, G.P. and Senior, C.L. "Identification of mercury species in unburned carbon from pulverized coal combustion." Proceedings of 92nd Air & Waste Management Association Annual Meeting, St. Louis, Missouri, June 20-24, 1999

17. Olson, E.S., Sharma, R.K., Miller, S.J. and Dunham, G.E. "Identification of the breakthrough oxidized mercury species from sorbents in flue gas." Proceedings of the Mercury in the Environment Specialty Conference, Minneapolis, Minnesota, September 15-17, 1999

18. Biswas, P. and Zachariah, M. "In-situ immobilization of lead species in combustion environments by injection of gas phase silica sorbent precursors." Environmental Science and Technology, 31, 2455-2463, 1997

19. Wu, C.Y., Lee, T.G., Arar, E. and Biswas, P. "Novel in-situ generated sorbent methodology and UV irradiation for mercury capture in combustion environments." Presented at the EPRI/DOE/EPA Combined Utility Air Pollutant Control Symposium, Washington D.C., August 25-29, 1997

20. Watras, C.J. and Huckabee, J.W. Mercury Pollution: Integration and Synthesis, CRC Press, Inc., Florida, P.3-19, P.621-628, 1994

21. Karr, C., Jr. Analytical Methods for Coal and Coal Products, Vol. HI, Academic Press, Inc., New York, P.489-541, 1979

22. Galbreath, K.C., Zygarlicke, C.J. and Toman, D.L. "Mercury-chlorine-fly ash interactions in a coal combustion flue gas." Proceedings of 91st Air & Waste Management Association Annual Meeting, San Diego, California, June 14-18, 1998

23. Lee, C.W, Kilgroe, J.D. and Ghorishi, S.B. "Speciation of mercury in the presence of coal and waste combustion fly ashes." Proceedings of 93rd Air & Waste Management Association Annual Meeting, Salt Lake City, Utah, June 18-22, 2000

24. Galbreath, K.C. and Zygarlicke, C.J. "Mercury transformations in coal combustion flue gas." Proceedings of Conference on Air Quality: Mercury, Trace Elements, and Particulate Matter, McLean, Virginia, December 1-4, 1998

25. Fan, M. Factors affecting the precision and accuracy of photoacoustic measurements of unburned carbon in fly ash, Ph.D. Dissertation, Iowa State University, Ames, Iowa, 2000

26. Sweterlitsch, J.J. Reduction of nitrogen oxides by biomass reburning, M.S. Thesis, Iowa State University, Ames, Iowa, 1999

27. Widmer, N.C., West, J. and Cole, J.A. "Thermochemical study of mercury oxidation in utility boiler flue gases." Proceedings of 93rd Air & Waste Management Association Annual Meeting, Salt Lake City, Utah, June 18-22, 2000

28. Dunham, G.E., DeWall, R.A. and Senior, C.L. "Fixed-bed studies of the interactions between mercury and coal combustion fly ashes." Proceedings of Air & Waste Management Specialty Conference on Mercury Emissions: Fate, Effects, and Control, Chicago, Illinois, August 21-23, 2001

29. Buonicore, A.J. and Davis, W.T. Air Pollution Engineering Manual, Van Nostrand Reinhold, New York, P.114-132, 1992

30. Operation and Maintenance Manual, Staclean Diffuser Company, Salisbury, North Carolina, 2000

31. Galbreath, K.C., Zygarlicke, C.J., Toman, D.L. and Schulz, R.L. "Effects of NO_x and α-Fe_2O_3 on mercury transformations in a 7-kW coal combustion system." Proceedings of 94th Air & Waste Management Association Annual Meeting, Orlando, Florida, June 24-28, 2001

32. Mamani-Paco, R.M. and Helble, J.J. "Bench-scale examination of mercury oxidation under non-isothermal conditions." Proceedings of 93rd Air & Waste Management Association Annual Meeting, Salt Lake City, Utah, June 18-22, 2000